PARTICLE PRODUCTION AT THE ISR

By E. Lillethun

University of Bergen*

(Presented at the XIII Cracow School of Theoretical Physics, Zakopane, June 1–12, 1973)

The paper is a review of the most recent data on particle production (mostly single particle inclusive production) at the CERN Intersecting Storage Rings. Discussed are total cross-sections, elastic cross-sections, production of π^+, K^+ and p^+ in the forward direction and in the large angle region, production of particles with large transverse momentum.

Introduction

My task as an experimentalist lecturing to an audience of theoreticians will at least be threefold, namely to bring to your attention the recent experimental results from the CERN Intersecting (proton) Storage Rings (ISR), to explain parts of the experiments in order to show why these results are limited in their spread over particles and other parameters and to stress possible difficulties in obtaining accurate data. The last part is rather important so that you should not spend too much time fitting data to a model — or a model to data — if the data suffer from large uncertainties.

The three points will not be covered in succession but rather mixed in with each other.

The ISR

In order to bring us into the picture of how the data are produced I want to give a short description of the ISR. For a more complete and very readable description of the ISR I recommend a recent article by Johnsen [1].

The layout of the rings, with their intersecting vacuum chambers and the proton supply lines from the CERN Proton Synchrotron (PS) is shown in Fig. 1. By tuning the PS and the ISR to the same proton momenta, a complete pulse of protons may be transferred into one of the ISR-rings where it is transferred to a more central position in the vacuum chamber. Several pulses are stacked in this way side by side until the beam is a band of a cross-section about 1 cm $\times$ 6 cm. This situation is sketched in Fig. 2, showing the crossing of the two beams and indicating the interaction region which is popularly called the diamond.

* Address: Institute of Physics, University of Bergen, Allegaten 53-55, N 5000 Bergen, Norway.

We note that the width of the beams correspond to a total momentum spread of about 2%. The value of centre of mass (cm) energy, $\sqrt{s}$, is always given with the energy corresponding to the central orbit but the particles then have a distribution which is essentially flat out to about $\pm 1\%$ of this. It is possible to use a more accurately determined momentum by measuring the position of the interaction within the proton band.

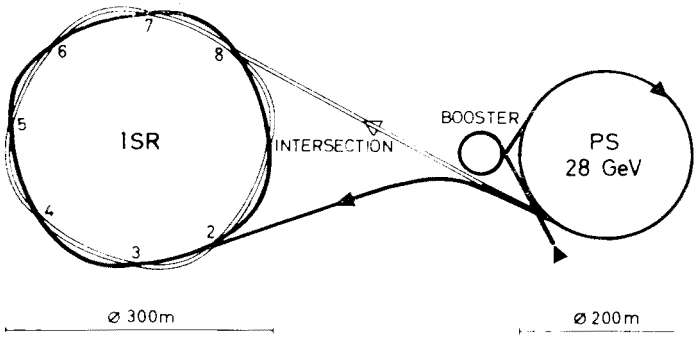

Fig. 1. Sketch of the CERN Intersecting Storage Rings

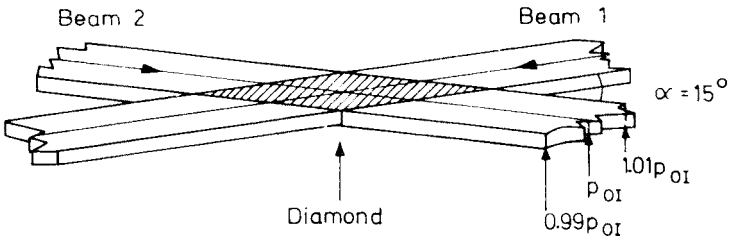

Fig. 2. Sketch of the intersecting proton-beams at the ISR

We note also that the crossing angle of 15° results in an unusual laboratory frame of reference. It may be specified by stating that the cm frame moves with a momentum of $2p_{OI} \times \sin 7°.5$ at right angles to the directions of the incoming protons, whose momentum is p_{OI}. The ISR laboratory frame and connected variables will in the following be labelled with the suffix I.

The ISR has been operated most of the time with "symmetrical" beams, *i.e.* with the same p_{OI} in each ring, with a choice of 4 values of p_{OI}. The values of p_{OI} and the corresponding values of s and $\sqrt{s}$ are given in Table I.

TABLE I

The usual ISR energies and some derived quantities

p_{OI}, GeV/c	s, GeV^2	$\sqrt{s}$, GeV	p_1, GeV/c	y_{max}
11.78	549.1	23.43	292	3.22
15.38	933.6	30.55	496	3.48
22.51	1996	44.67	1060	3.86
26.59	2784	52.76	1480	4.03
(31.6)	(3936)	(62.8)	(2100)	4.21

It should be mentioned that the ISR rather early was run a few times at momenta lower than 11 GeV/c, and that runs at a momentum of 31 GeV/c have been made possible after acceleration of the proton beams within the ISR.

Before leaving the ISR itself I want to express my admiration for the way the ISR team has pushed the operation of the machine towards perfection. By now the ISR has operated with a collision frequency (luminosity) higher than designed, it has on the average

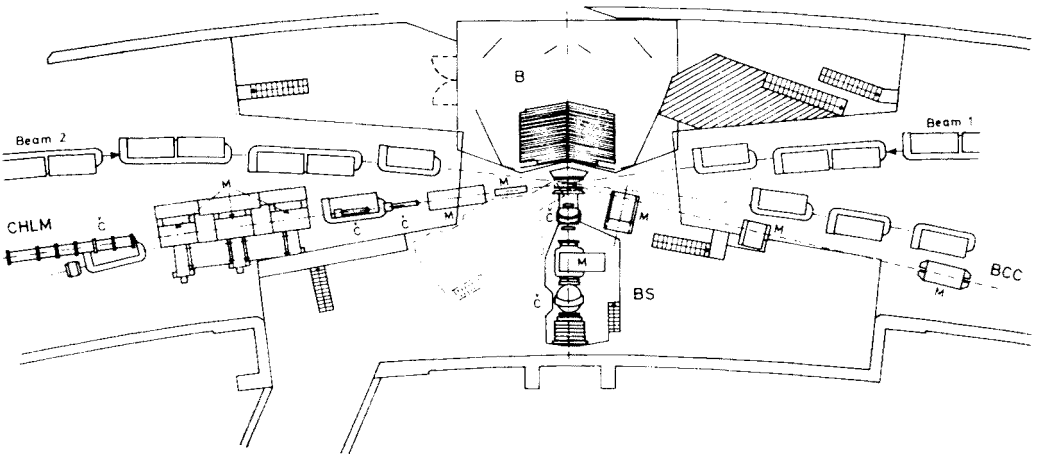

Fig. 3. Sketch of the Intersection 2 at the ISR. BCC, B, BS and CHLM indicate the experimental equipment of the Bologna–CEN–CERN group, the British Universities Collaboration, the British–Scandinavian Collaboration and the CERN–Holland–Lancaster–Manchester group respectively. M = bending magnet, Č = Čerenkov counter

a vacuum of better than 10^{-10} torr (*i.e.* about 3500 H_2 molecules per mm^3) and it has kept the beams running for 46 hours continuously with a reduction of only 60 % in luminosity during this period.

What an achievement: Each proton was kept within about 1 cm^2 of its central path for a distance of almost two lightdays!

Experimental setups

As could be seen from Fig. 1, the proton beams cross each other in 8 intersecting regions. Apart from regions 3 and 5 all regions are now in use for experiments. Most of the measurements on identified charged particle production has been performed in intersection region 2.

The groups involved are the Bologna–CEN–CERN (BCC) group and the Bologna–Michigan (BM) group for measuring particle production at intermediate angles (80 mrad $\lesssim \Theta_1 \lesssim$ 300 mrad), the British–Scandinavian collaboration (BS) measuring at large angles ($45^\circ < \Theta_1 < 90^\circ$) and finally the CERN–Holland–Lancaster–Manchester (CHLM) group measuring at small angles (25 mrad $< \Theta_1 <$ 150 mrad). The layouts for these experiments are shown in Fig. 3.

In interaction region 1 the Saclay–Strasbourg (SS) group has measured particle production at 90° and the CERN-Columbia Rockefeller (CCR) group measured π^0 production.

During the earlier running of the ISR some groups measured angular distributions of charged particles with no determination of particle type or momentum. Included here are the groups using the emulsion technique, among others the group at Cracow. These groups have been located in the intersection regions 1, 4, and 6. In region 8 the Pisa-Stony Brook (PSB) group measures total cross sections with equipment which also allows measurements of angular distributions of charged particles almost over the complete solid angle of 4π, but unfortunately without particle identification and momentum measurement.

The experiments will be described in more detail in the following only in so far as it is necessary for the understanding of some aspects of the data.

Kinematics, symbols, definitions

At ISR we are concerned with proton-proton collisions. We are in particular interested in inclusive reactions $p+p \rightarrow c+X$, where c is the particle measured and X is anything, or if you want to, the missing mass in the measured reaction.

In most cases we are talking about the parameters of c, such as its momentum p, energy E, mass m and the production angle Θ. We shall let p and m represent pc and mc^2, and use the suffix 1 if we refer to the usual laboratory frame, *i.e.* the frame with a stationary target. No suffix will be used in the cm system.

Fig. 4 shows the three systems used and gives some of the transformations between the systems. A more complete treatment of the transformations from the ISR system to the cm system can be found in Ref. [2].

In order to define what we are studying, let me quote Fermi [3] from 1950: "When two nucleons collide with very great energy in their center of mass system this energy will be suddenly released in a small volume surrounding the two nucleons. We may think pictorially of the event as of a collision in which the nucleons with their retinue of pions hit against each other so that all the portion of space occupied by the nucleons and by their surrounding pion field will be suddenly loaded with a very great amount of energy".

This picture is still useful, although the "retinue of pions" now gets the name of partons, stuff, quarks *etc.* Fermi's paper was the beginning of hadron thermodynamics, to which Hagedorn's [4] name is closely linked. Another approach to the particle collisions is Landau's hydrodynamical model [5] which recently is being brought forward again by Carruthers and Duong-van [6]. Still other models are the multiperipheral interaction [7], the bremsstrahlung model of Feynman [8] and the hypothesis of limiting fragmentation of Yang [9]. From all these models we can make our own simple picture which is useful enough for the discussion of the data.

As a proton is "accelerated" from, say, 10 GeV to 30 GeV its velocity hardly changes ($\Delta\beta/\beta \sim 5^0/_{00}$), *i.e.* it is hardly accelerated. But its energy and momentum, and as some people would say, its relativistic mass are tripled. The proton being accelerated is more like a growing drop of energy at essentially constant velocity. Or we could compare it to a growing region of "ability to produce particles" with some momentum.

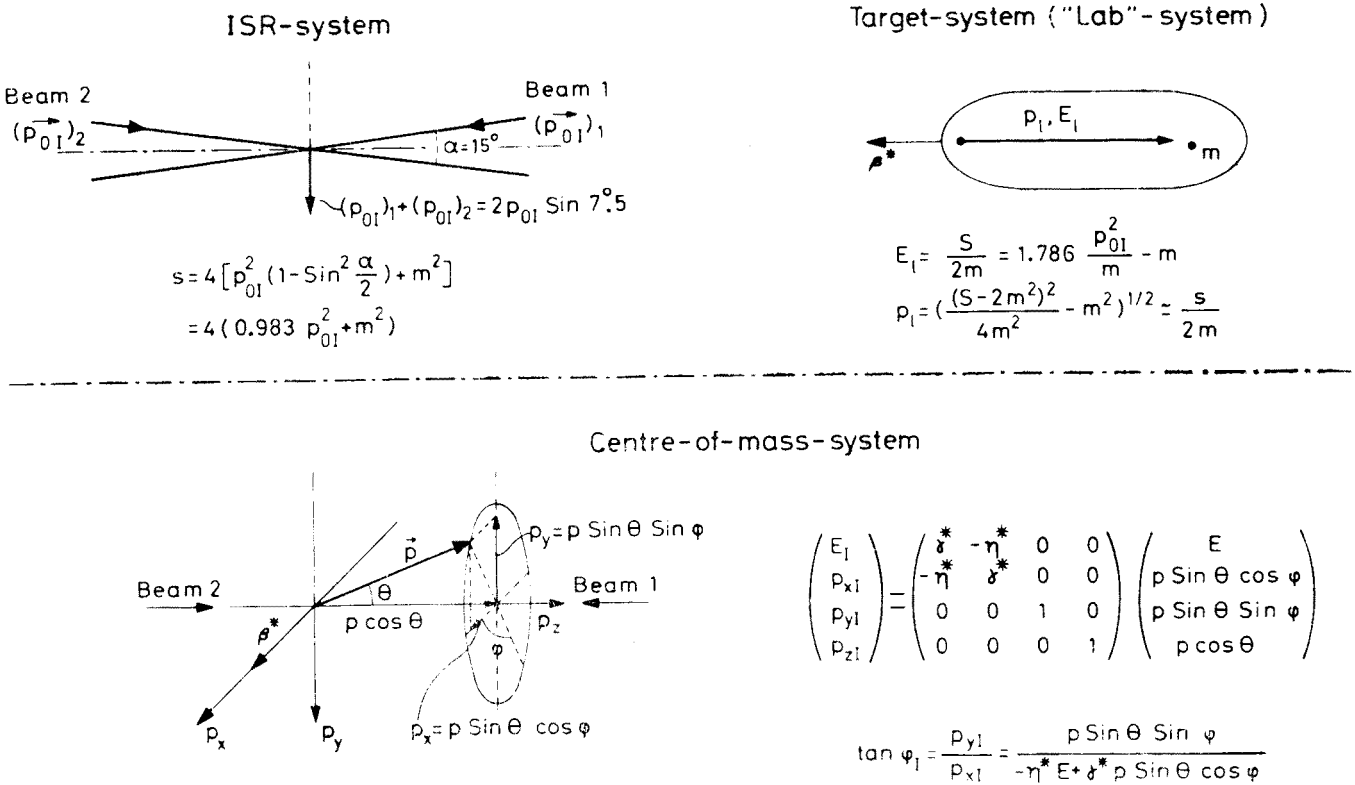

Fig. 4. Sketch showing some of the reference systems used with indices and some transformation properties. The asterisk signifies a quantity connected to the motion of the complete centre-of-mass system

When this drop encounters another particle it breaks open, (Fig. 5) bits and pieces flying in all directions and with different energies. The relevant function for the cross-section for particle production is the invariant $F(p, s) = Ed^3\sigma/d^3p$ giving statistically the produced particle energy density per unit momentum space.

Now, we know that the average transverse momentum p_T of the produced particles is small, while the longitudinal momentum p_L can be large. In general the distribution

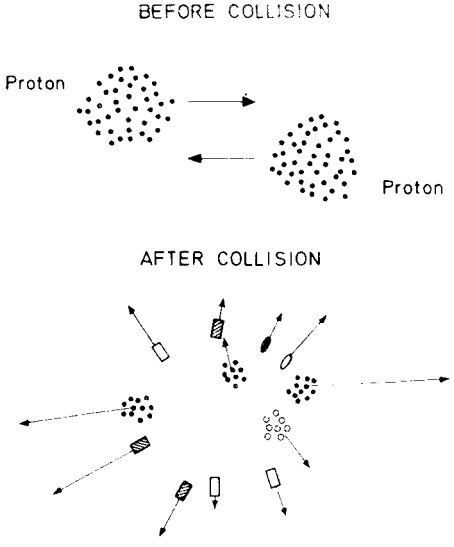

Fig. 5. The author's concept of a proton-proton collision, seen in the centre-of-mass system

of particles according to p_T is not very strongly dependent on p_L so we study the variation of F with respect to p_T or p_L independently. As a matter of fact, instead of p_L one chooses the Feynman variable $x = 2p_L/\sqrt{s}$ or the rapidity

$$y = \frac{1}{2}\ln\frac{E+p_L}{E-p_L} = \ln\frac{E+p_L}{(p_T^2+m^2)^{\frac{1}{2}}};$$

$\sqrt{p_T^2+m^2}$ is called the longitudinal mass. Another way of looking at this quantity is to call it the transverse energy E_T, because when $p_L \gg m$ we may regard p_L as a longitudinal energy E_L and the total energy for a particle would be $E = E_T^2+E_L^2 = p_L^2+p_T^2+m^2$. The rapidity is a very useful variable. We find for example that $F = d^3\sigma/dyd^2p_T$ and that y transforms simply under a Lorentz transformation along the longitudinal direction. For example, to transform to a system (s) moving with velocity βc with respect to the cm system we find for y': $y' = y-y_s$, where $y_s = \frac{1}{2}\ln[(1+\beta)/(1-\beta)]$.

Total cross-sections

Some of the most interesting results from the ISR are the data showing the increase of the total proton-proton cross section with increasing energy [10–12]. The results are

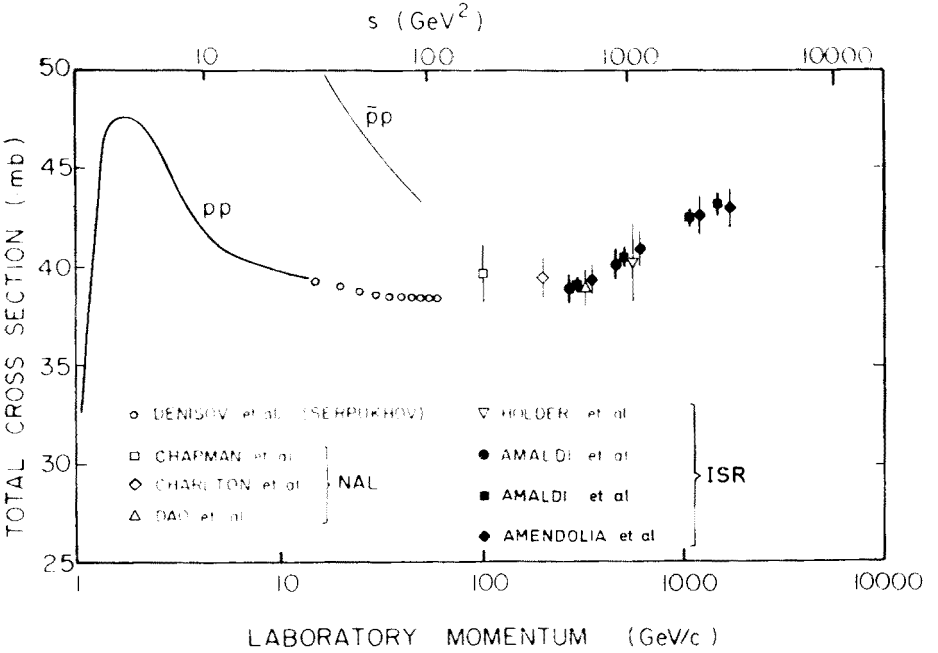

Fig. 6. The total proton-proton cross-section as function of the square of the centre-of-mass energy, s, and the corresponding laboratory proton momentum. The proton-proton and antiproton-proton cross-sections for lower energies are indicated by curves only. The ISR references see Ref. [16]

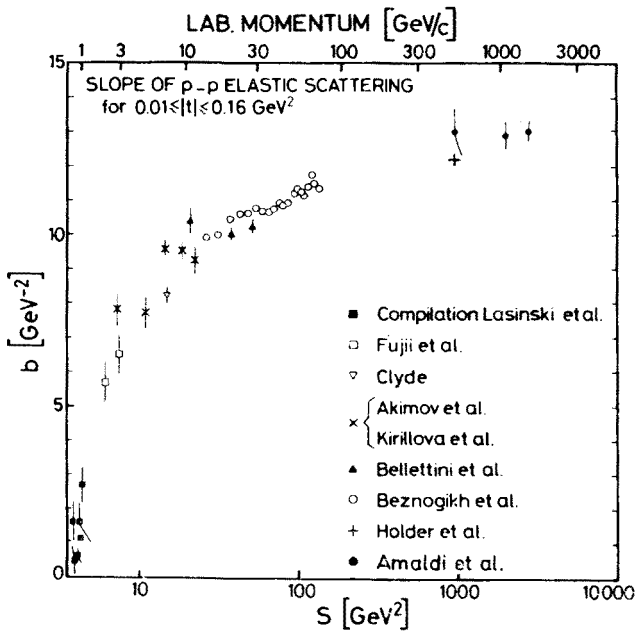

Fig. 7. The slope parameter b for $t < 0.16\ \mathrm{GeV}^{-2}$ as function of the square of the centre-of-mass energy, s, for elastic proton-proton scattering. b is defined by the form $d\sigma/dt = A \exp(bt)$

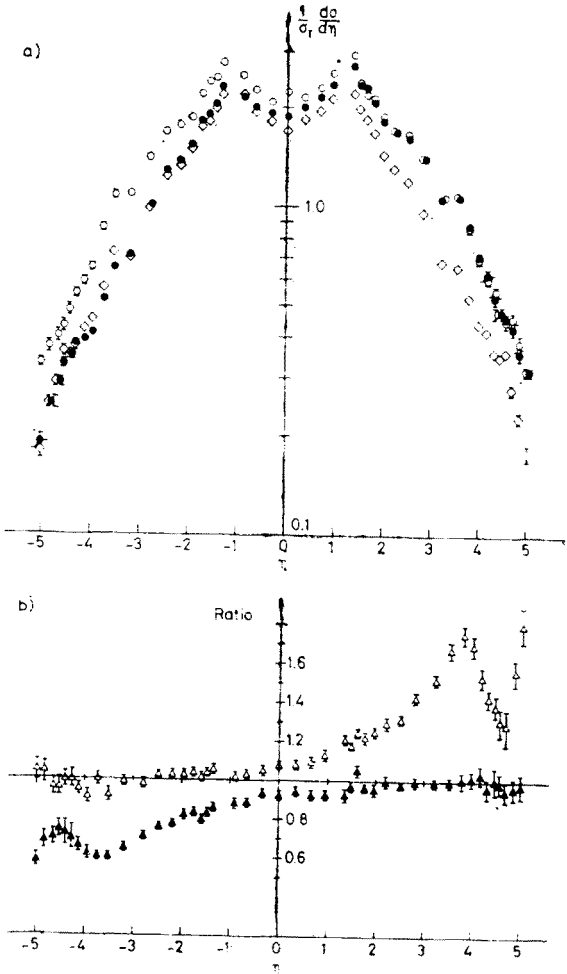

Fg. 8 a) Single particle inclusive density distributions $(d\sigma/d\eta)\ \sigma_T^{-1}$ as function of $\eta = -\ln \tan \Theta/2$ for prioton proton collisions with the following momenta for the two protons. Run 1: $(p_{OI})_1 = (p_{OI})_2 = 15.4$ GeV/c; Run 2: $(p_{OI})_1 = (p_{OI})_2 = 26.6$ GeV/c; Run 3: $(p_{OI})_1 = 15.4$ GeV/c, $(p_{OI})_2 = 26.6$ GeV/c. b) Ratios of the above density distributions for asymmetric and symmetric proton momenta as function of η. Upper points from Run 3 and Run 1 and lower points from Run 3 and Run 2. The data are from Ref. [16]

shown in Fig. 6. Indeed, it looks as if the proton is growing with energy. The experimental data are within errors in agreement with the maximum increase with energy allowed by unitarity, the Froissart limit [13].

Elastic cross-sections

The shrinking of the diffraction scattering peak has been shown to continue from PS energies to ISR energies [14, 15], although with a slower rate of shrinking than at the lower energies. A compilation of the results on the value b, from the fitting of the dif-

fraction peak to $d\sigma/dt = \exp(bt)$, as taken from Ref. [15], is shown in Fig. 7. The continued shrinking shows, in terms of the optical model picture, that the proton "radius" still increases with energy. It should be noted that the shrinking of the diffraction pattern is large already at energies where the total cross-section is roughly constant.

Production of particles

Let us start our study of the particle production data by looking at the results of the PSB group [16] (see Fig. 8). The measurement consists of recording the angle of production of each charged particle but without identification of charge, mass or momentum. The

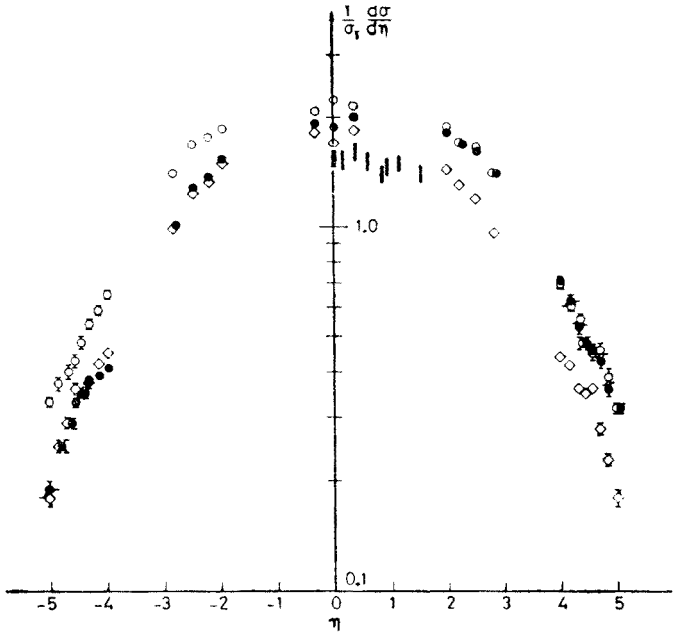

Fig. 9. Same distribution as in Fig. 8a, but structures in the distributions caused by secondary particles produced by extra material in the apparatus have been removed by the author. The number of points removed have been chosen according to the author's feelings! Data are from Refs [16] and [17]

group explains that the structure in the data is instrumental. I have therefore shown the data again in Fig. 9 where these regions have been omitted. I warn you that the widths of the cutouts have been chosen by my own feeling for which regions are clean. For comparison I have also included some of the data of the Cracow–CERN [17] group in Fig. 9.

Two sets of the PSB data points, given as $\sigma_T^{-1} dN/d\eta$ *vs* η, are from symmetric momenta in the ISR, namely 15.4 GeV/c in each beam or 26.6 GeV/c in each beam. A third set of data points are recorded with one beam at 15.4 GeV/c and the other at 26.6 GeV/c. The striking feature of the data is that the distribution of particles in the forward cone for the incoming proton remains the same whether the proton it collides with (the target proton) has a momentum of 15.4 or 26.6 GeV/c. We may think of the target proton to

act only as a tool for breaking open the incoming proton, letting its bits and pieces spray out according to a distribution inherent in its state of energy. We note that for the incoming proton nothing is changed between the symmetric and asymmetric runs. The angles measured in the ISR frame are relative to this beam axis and when the protons along this beam axis in both experiments have the same momentum, the coordinate system remains un-

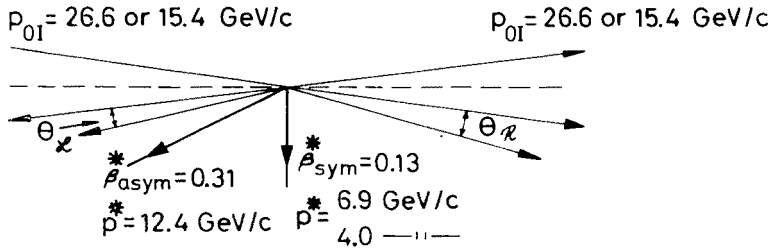

Fig. 10. A sketch indicating the changes in the motion of the centre-of-mass system (indicated by asterisks) from symmetric to asymmetric proton momenta

changed for the incoming proton. This is not so for the cm systems. The change in their motion is sketched in Fig. 10. See also Table II.

I believe the most important conclusion from this experiment, if the equality between the distributions in the fragmentation region is taken to be absolute, is that a high energy proton does not care about how hard it was hit by another proton. It produces in any case the same forward angular distribution in a frame obtained by some fixed Lorentz transformation of its rest frame along its direction of motion.

TABLE II

ISR energies for asymmetric beam energies

$(p_{01})_1$, GeV/c	26.6	26.6	15.4	(22.5)
$(p_{01})_2$, GeV/c	26.6	15.4	15.4	(22.5)
s, GeV^2	2784	1610	934	(1996)
$\sqrt{s}$, GeV	52.8	40.2	30.6	(44.7)

Up to this point no approximations have been brought into the picture. We use the directly measured values. In their paper the PSB group introduces the rapidity in order to show that the data are consistent with the Hypothesis of Limiting Fragmentation (HLF) [9].

The approximations needed are the following:

(*i*) The HLF describes distributions in the laboratory frame (target or projectile frame). The ISR system is closer to the cm system and the transformation to the laboratory system is impossible because of lack of knowledge about the particles. The group claims that the ISR system is a good enough approximation to the cm system, and the transformation from the cm to the lab system is then a finite boost in y which should not change the y-distributions.

(*ii*) The relationship between η and y is for our purpose most readily seen from the following formulae

$$\eta = -\ln\tan\frac{\Theta}{2} = \frac{1}{2}\ln\frac{p+p_L}{p-p_L} = \ln\left(\frac{p+p_L}{p_T}\right),$$

$$y = +\frac{1}{2}\ln\frac{E+p_L}{E-p_L} = \ln\frac{E+p_L}{(m^2+p_T^2)^{\frac{1}{2}}} = \ln\frac{p\left(1+\left(\frac{m}{p}\right)^2\right)^{\frac{1}{2}}+p_L}{p_T\left(1+\left(\frac{m}{p_T}\right)^2\right)^{\frac{1}{2}}}.$$

It is clear that when $(m/p_T)^2 \ll 1$ the two expressions approach each other. From other experiments we know for example that $\langle p_T\rangle \sim 300$ MeV/c for pions. Therefore a large amount of the particles are produced in regions where $(m/p_T)^2 \sim 1$ and the approximation is not so good. Particles with $p_T < m$ in the central region I believe are absorbed both in the ISR vacuum pipe and the first scintillator(s) and do therefore not disturb the picture, but on the other hand the particle momentum cutoff may be a bit arbitrary. In the very small angle region where p_T would be small even for large p, *i.e.* for $|y| > 5$, equivalent to $\Theta \sim 13$ mrad, the particles cannot be detected and we get the cutoff in the distribution at this value of y.

The group has looked into the effects of a substitution of y for η for their data and find the changes so small that the results can be taken as a proof of the HLF.

I have spent a lot of time discussing these data even if the measurements give only number of particles as function of angle, because they introduce a nice overall picture of the situation. We shall now continue to look at data where particles are clearly identified and the momenta measured. Because these experiments need much more equipment per solid angle, different regions have been explored by different groups.

I shall first discuss the experiments and the results of some of these groups and in the end give the resulting overall data picture for the different particles.

Production of π^-, K^- and $p^\perp$ in the forward direction

The experimental setup of the CERN–Holland–Lancaster–Manchester group is shown schematically in Figs 3 and 11. Their measurements [18, 19, 20] cover both negative and positive particles in an angular range 25 mrad $< \Theta <$ 180 mrad, with the angle lying in the vertical plane.

In Ref. [18] the group has chosen to measure the production of negative particles as a function of fixed cm angles, chosen so that the x and p_T regions for different $\sqrt{s}$ overlap. The choice of angle was defined by $p_T/p_L = \tan\Theta = 2.66(s)^{-\frac{1}{2}}$ resulting in the relationship $p_T = 1.33 \cdot x$.

The results are reproduced in Figures 12 a, b and c. For π^- they observe such a perfect scaling within the ISR energy range that only the set for $\sqrt{s} = 52.8$ GeV is shown, together with points representing data of Allaby *et al.* [21] taken at $\sqrt{s} = 6.8$ GeV. Up to $p_T = 0.5$ GeV/c there is perfect scaling within this large energy interval. The scaling breaks

down more and more for the higher p_T (and x) values. The limit of phase space for $\sqrt{s} = 6.8$ GeV is at $x \sim 0.85$ so the non-scaling probably is caused by this (see below).

The spectra for K^- and p^- also show scaling within the ISR energies, but now the measuring errors are larger, of the order of 10 to 20%. No systematic trend for non-scaling within ISR energies is seen. However, the invariant cross-sections at PS energies are lower

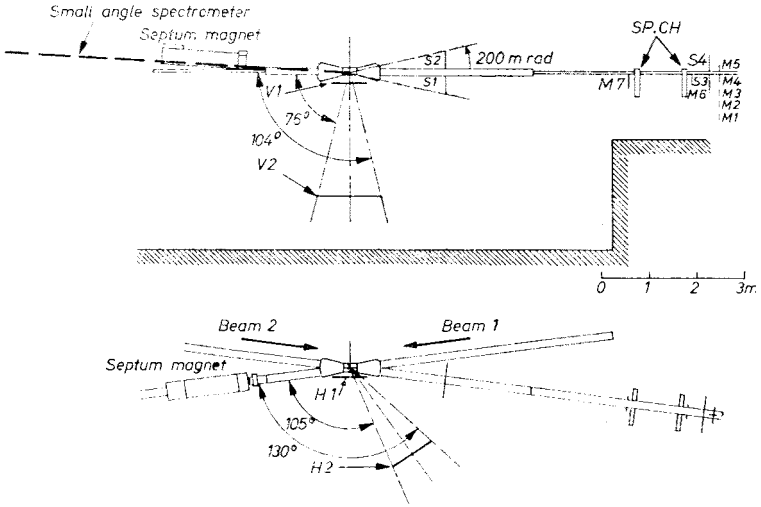

Fig. 11. Schematic drawing of parts of the experimental setup of the CHLM-group. The line in the upper left corner represents small-angle scattered particles extracted by means of a septum magnet. The particles are further analysed by a spectrometer and Čerenkov counters shown in Fig. 3. In addition are shown the counter hodoscope M1–M5, telescope 1 (V1 and V2) below the diamond, telescope 2 (H1 and H2) in the horizontal plane, centered at 117°, 5 and telescope 3 around beam 2 (S1–S4, M1–M7 and two spark chambers)

by factors of 2 and 6 for K^- and p^- respectively for p_T around 0.4 GeV/c, and considerably lower for higher p_T. The antiproton data show also a marked difference in behaviour at low p_T, where the PS data flatten off and the ISR data still rise essentially exponentially.

In Ref. [19] the CHLM group presents data on both positive and negative particles, but now for $\sqrt{s} = 52.8$ GeV at fixed values of x, showing the p_T spectra. Since the data are already published I shall only give some of the conclusions and include some of the cross-sections in the combinded data plots (Figures 20 and 21).

(*i*) All the data can be well fitted with the form $F = A \exp(-Bp_T^2)$ with B decreasing with the mass of the particle, *i.e.* the average transverse momentum $(= (\pi B)^{-\frac{1}{2}})$ increases with particle mass.

(*ii*) Scaling between PS and ISR energies is on the average good for $\pi^{\pm}$ and K^+, but the ISR data show some structure which is not found in the PS data. The CHLM group does not comment on this and one is therefore led to believe that the structure may be instrumental. Neglecting this structure one finds that for $x = 0.18$ and $x = 0.21$ the PS and ISR data are consistent with scaling up to $p_T = 1.0$ GeV/c. Comparing this to the data

in Ref. [18] we see that the deviation from scaling noticed there is due to the larger x-values connected to the larger p_T values.

(*iii*) K^- and $p^{\pm}$ cross-sections at ISR differ by large factors ($\sim$2 to 5) from the PS data, with the proton cross-sections at the ISR energies lower than those at PS energies.

The CHLM group has made a special effort to measure the inelastic proton spectrum at high values of x [20]. At $x = 1$ protons will to a large extent be elastically scattered and the experimental equipment had to be elaborated in order to separate the elastic from the inelastic events.

As shown in Fig. 11 five counters ($M_1 - M_5$) were placed on top of and below the downstream beamline opposite the spectrometer (Beam 2). M_3 was centered on the same angle Θ as the spectrometer. Whenever an elastic proton is recorded in the spectrometer the other proton should hit M_3. If in the collision the mass of the beam 2 particle was increased, its "decay" proton should be found distributed in an angular cone around the direction defined by the elastically scattered protons.

The separation of the two types of events is shown in their paper to be clear and I reproduce two of their data sets in Figures 13 a and b. Fig. 13 a shows both the elastic and the inelastic proton distributions for $14.5\ \text{GeV}/c < p < 15.5\ \text{GeV}/c$ ($0.94 < x < 1.01$) where $p_{OI} = 15.4\ \text{GeV}/c$. Due to the experimental resolution the data points go beyond the elastic limit.

The only slightly disturbing fact about the separation is that although the authors claim that the elastic peak is symmetric, the data reveal a tendency toward a tail on the low momentum side, a factor 3 to 4 lower than the inelastic value. The tail may cause some error in the quantitative estimate of the inelastic cross-section, but does not affect the main trends of the data.

Fig. 13b displays the inelastic proton production spectra for $0.5 < x < 1.0$ and for three values of p_T^2, *viz.* 0.275, 0.525 and $1.05\ (\text{GeV}/c)^2$ and some points for $p_T^2 = 1.755\ (\text{GeV}/c)^2$. The three data sets clearly show a peak close to $x = 1$ which is interpreted as the diffraction excitation of the beam 2 proton to an isobar which subsequently decays. Similar data were also presented earlier [22].

We summarize the conclusions in the papers:

(*i*) The invariant cross-section for inelastic proton production for $0.5 < x < 1.0$ and $0.8 < p_T < 1.0\ \text{GeV}/c$ scale between $\sqrt{s} = 30.5$ and $\sqrt{s} = 44.7\ \text{GeV}$.

(*ii*) A peak seen in the inelastic proton spectrum close to $x = 1$ indicates the production of states with masses up to at least 7 GeV. The resolution is not sufficient to indicate specific states.

Another measurement of the production of charged particles in the relatively small angle region ($80 < \Theta < 300$ mrad) is reported by the BCC group [23, 24]. Their spectrometer recorded particles with momenta between 1.5 GeV/c and 10 GeV/c. The observed particles emerged in the horizontal plane and the momentum resolution is about $\pm 4\%$ for the usual setup and $\pm 11\%$ for a shorter setup used for detecting kaons with reduced decay corrections. The group quotes over-all errors of about 10% for pions and protons and 10–25% for kaons and antiprotons. In many cases the data points scatter by more than what should be expected from these over-all errors. This may indicated an underes-

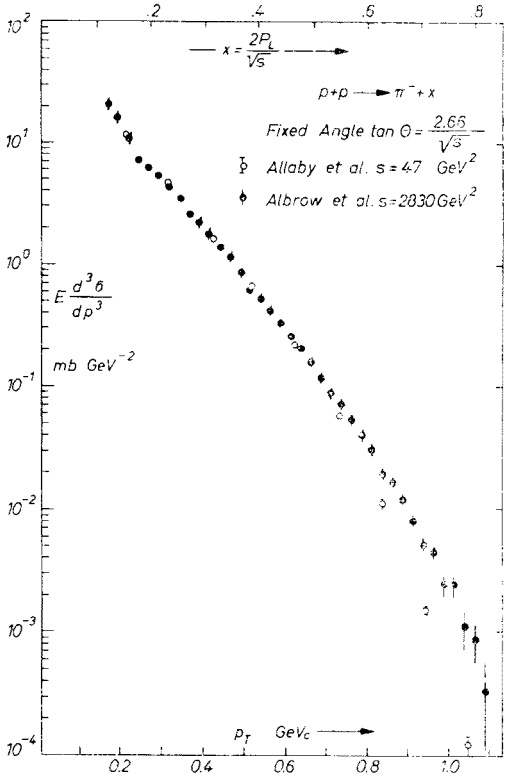

Fig. 12a

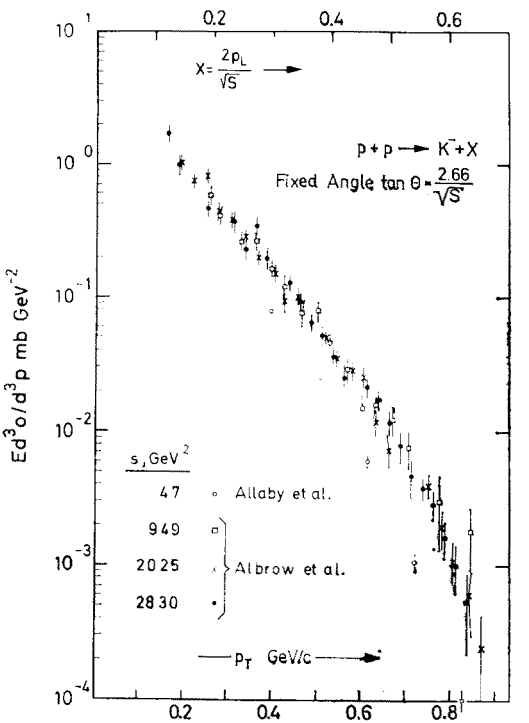

Fig. 12b

timate of the uncertainties in the background subtraction or the luminosity measurements.

Data are presented for all the usual ISR energies for the following values of p_T and x:

$\pi^\pm, K^\pm, p^\pm$: $x = 0.15,\ 0.2 < p_T < 1$ GeV/c;

$p^\pm$: $x = 0.08,\ 0.2 < p_T < 0.6$ GeV/c;

$p^\pm$: $x = 0.32,\ 0.4 < p_T < 1.4$ GeV/c;

$\pi^\pm, K^\pm, p^\pm$: $p_T = 0.2,\ 0.4,\ 0.8$ and 1.2 GeV/c with varying intervals of x between 0.07 and 0.4.

The same general features concerning scaling hold for these data as for the data of the CHLM group, partly overlapping in x and p_T values:

(*i*) Scaling between PS and ISR energies is well established for pions of $p_T < 0.8$ GeV/c.

(*ii*) Deviations from scaling are greatest for large p_T and small values of x for all particles.

To demonstrate these effects we show the x-distributions for $K^\pm$ and p^- in Fig. 14. We notice that for $x < 0.2$ the cross-sections for fixed p_T rise much more rapidly than seems

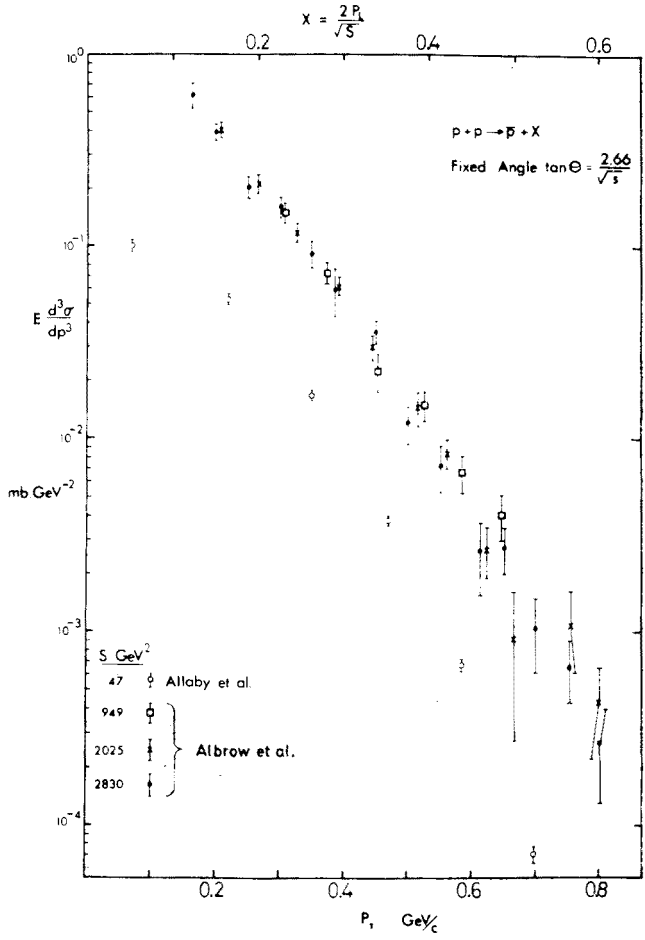

Fig. 12. The invariant cross-section for production of π^-, K^- and p^- in collisions as function of the transverse momentum, p_T, and $x = 2p_L/\sqrt{s}$ with $\tan\Theta = 2.66\ (s)^{-\frac{1}{2}}$. The data are from the CHLM group, Ref. [18] and Allaby *et al.*, Ref. [21], a), b) and c) show the data for π^-, K^- and p^- respectively. The square of the centre-of-mass energies are given in the figures

to be indicated by the PS data. We shall come back to discuss this in connection with the large angle data in the next Chapter.

In its report the group has also worked out the multiplicities for $\pi^\pm$, $K^\pm$ and $p^\pm$ under the assumption that the invariant cross-section for constant y follows the exponential law $Ed^3\sigma/d^3p = A \exp(-Bp_T)$ for all y and that the y-distribution ($g(y)$) is given by the cross-sections measured by the different groups at $p_T = 0.4$ GeV/c. The values chosen for B are 6.0 (GeV/c)$^{-1}$ for $\pi^\pm$, 5.0 (GeV/c)$^{-1}$ for $K^\pm$ and 4.0 (GeV/c)$^{-1}$ for $p^\pm$. No reason has been given for this choice, and although it may be a fair choice in the central region, the CHLM data [18] for fixed Θ ($y \sim$ constant) in the fragmentation region indicate B

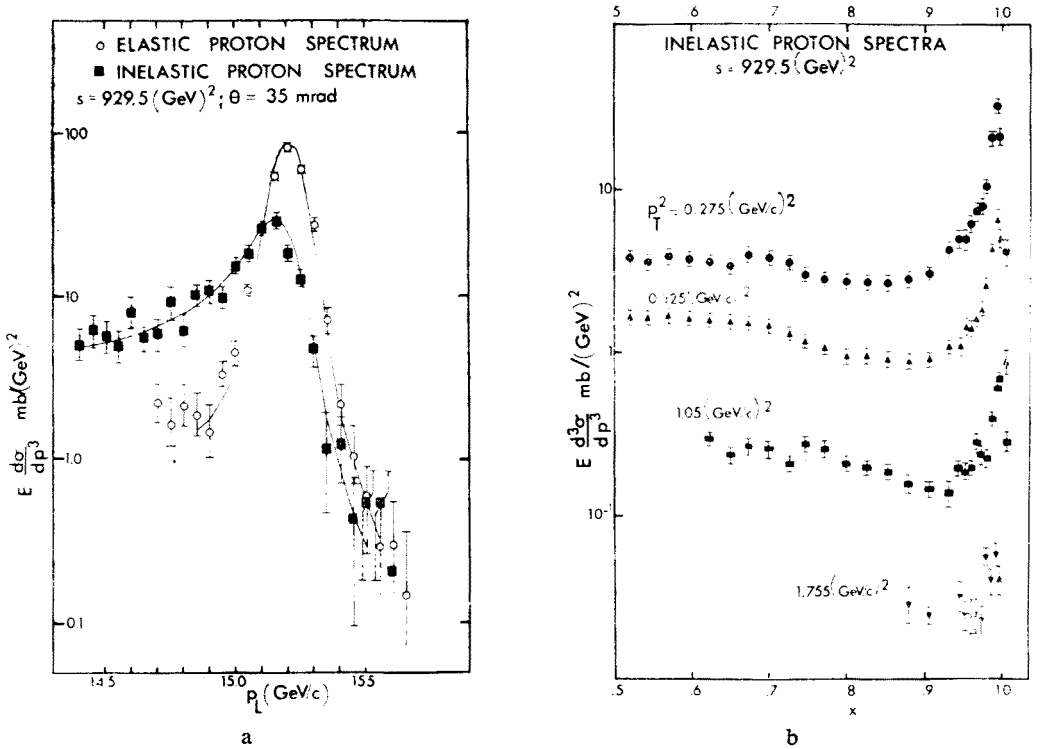

Fig. 13. The invariant cross-section for protons in proton-proton collisions of centre-of-mass energy $\sqrt{s} = 30.6$ GeV. $\Theta = 35$ mrad. In a) are shown data on both elastic and inelastic protons as function of the longitudinal momentum, p_L. In b) are shown data on inelastic protons as function of $x = p_L/\sqrt{s}$ for $p_T^2 = 0.275$, 0.525, 1.05 and 1.75 $(\text{GeV}/c)^2$. The data are from the CHLM-group, Ref. [20]

closer to 10 $(\text{GeV}/c)^{-1}$ than 6 $(\text{GeV}/c)^{-1}$ for π^-. For these data an exponential fit is not very good in any case.

I refer the reader to their paper for the multiplicities obtained.

Production of π^-, $K^\pm$ and $p^\pm$ in the large angle region

The new data in this region come from the BS group [25–27]. The experimental setup is mounted on a platform which can be rotated between 36° and 90°. Protons and antiprotons can be separated from the other particles up to momenta of about 1.2 GeV/c, while pions can be separated from kaons up to about 1 GeV/c. The kaon cross-sections are not measured beyond $p \sim 0.6$ GeV/c because of the large corrections due to mixing with the much more abundantly produced pions.

One should be aware of the following difficulties in the data reduction:

(*i*) The pion-spectra include pions coming from the decay of K^0. No correction has been made for this, but the effect has been estimated to be less than 5% in the quoted cross-sections. The main contribution of these pions may be for the low values of momentum.

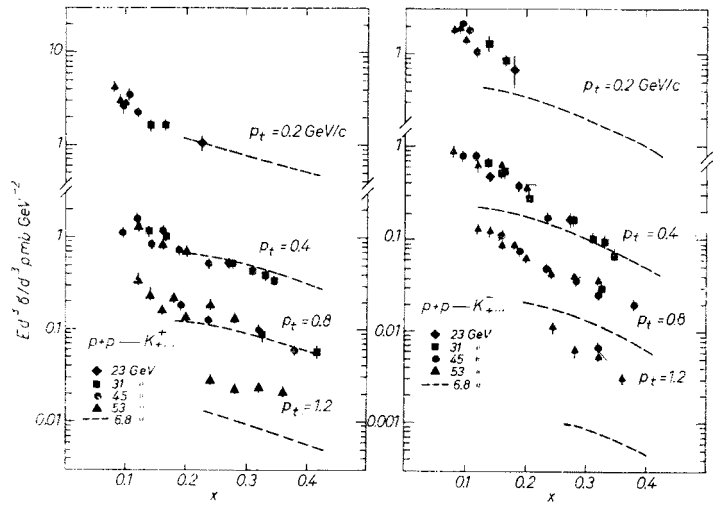

a

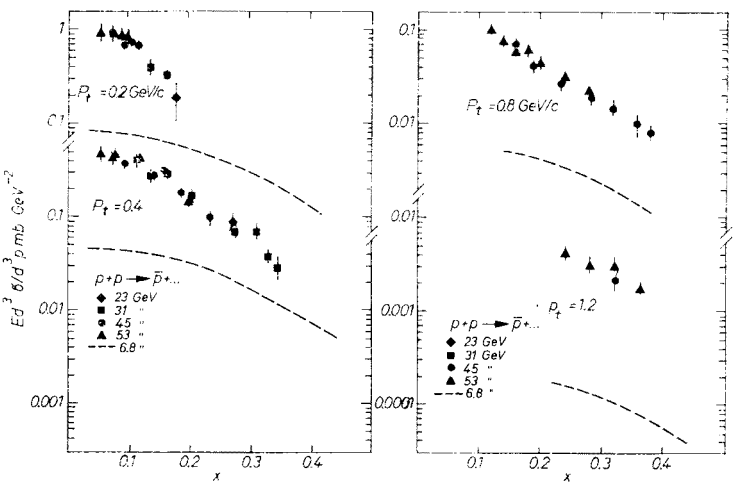

b

Fig. 14. The invariant cross-section for production of K^+ and p^- as function of $x = 2p_L/\sqrt{s}$ for transverse momenta p_T = 0.2, 0.4, 0.8 and 1.2 GeV/c. The centre-of-mass energies are indicated in the figure. The data are from the BCC-group, Ref. [23] and [24] and the dashed lines represent the data of Allaby *et al.*, Ref. [21]. The data for K^+ and K^- are shown in a) the data for p^- in b)

(*ii*) The background of particles from beam-gas and beam-wall collisions is in general very small, but for protons of low momenta the background can be rather high (worst case is $\sim$ 40% background for p_T = 0.2 GeV/c in one case).

(*iii*) Although the experimental setup on the platform is symmetric, the angular acceptance depends on momentum and the sign of the particle charge. Hence the angles quoted are only nominal central values, while the y-values computed are the correct ones.

But, some data have been taken with reversed magnet polarity, and the cross-sections quoted are given for the average y-value, which in the extreme case can be the average from ± 0.1 in y. Because of the slow variation of the cross-sections with y, this is not very important, but may tend to scatter the points somewhat unsystematically about in the y-plots. In general measurements have been made for $\Theta_I = 89°$, $75°$, $62.5°$, $45°$ and $36°$.

(*iv*) If the present data for $\pi^{\pm}$ are compared with those of the Saclay-Strasbourg group one finds an increasing discrepancy with increasing p_T. This is attributed to the data

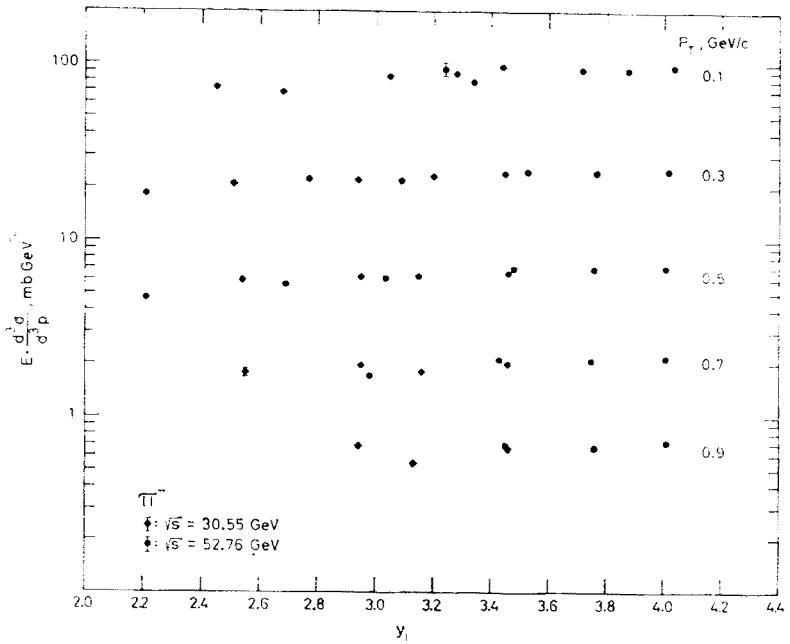

Fig. 15. The invariant cross-section for production of π^- as function of $y_1 = y_{max} - y$, for centre-of-mass energies 30.6 and 52.8 GeV and transverse momenta $p_T = 0.1$, 0.3, 0.5, 0.7 and 0.9 GeV/c. The data are from the BS-group, Ref. [26]

reduction of the SS group. Kaons could not be separated from pions, so an estimated kaon cross-section was subtracted from the total. Later measurements have shown that the estimated cross-sections were too low.

The pion data show the following:

(*i*) Plots of F *vs* $y_1 = y_{max} - y$ show for each energy ($\sqrt{s} = 30.6$ GeV and $\sqrt{s} = 52.8$ GeV) a slight increase with y_1. The increase is such that data from the two energies within errors agree in the overlap regions. Although the slope of a curve through the points must be 0 at y_{max}, the data have been fitted to $(F)p_T = A \exp(-Dy)$ to indicate the increasing cross-section. D is found to be 0.15 ± 0.03, corresponding to an increase of about 16% for each unit in y. The data for π^- are shown in Fig. 15.

(*ii*) Consistent with the results mentioned under (*i*) there is an energy dependence for F at fixed p_T even at ISR energies. For $p_T = 0.4$ GeV/c the cross-sections are plotted in Fig. 16 together with data from Mück *et al.* [28]. In Fig. 16 it is seen that the data

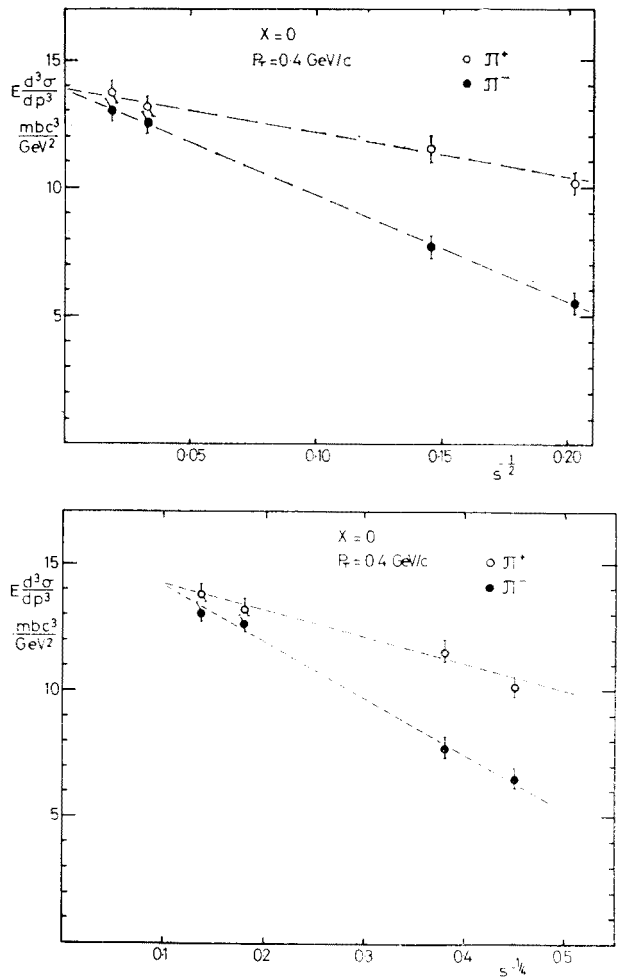

Fig. 16. The invariant cross-section for production of π^+ and π^- at $\Theta = 90°$, of transverse momentum $p_T = 0.4$ GeV/c as function of $s^{-\frac{1}{2}}$ and $s^{-\frac{1}{4}}$. The data are from the BS-group, Ref. [25] and Mück *et al.*, Ref. [28]

can be fitted on straight lines as function of $s^{-\frac{1}{2}}$ and that the π^+ and π^- cross sections then will meet at $s = \infty$. Fig. 16 shows also that the data are inconsistent with a $F \propto s^{-\frac{1}{4}}$ as has been suggested by Ferbel [29].

(iii) The p_T interval covered changes with angle since the total momentum measured is restricted: $0.13 < p_T < 1.05$ GeV/c at $\Theta_I = 89°$ and $0.11 < p_T < 0.60$ GeV/c at $\Theta_I = 36°$. Data have been collected for several runs with different trigger modes, and Table III lists the data in the form of fits to exponential forms. The functional forms should not be used to extrapolate the data outside the ranges of p_T indicated.

(iv) As shown in Fig. 17 the ratio of positive to negative pions is nearly 1.00 for small values of p_T, rising with increasing values of p_T to 1.17 for $p_T = 1.0$ GeV/c.

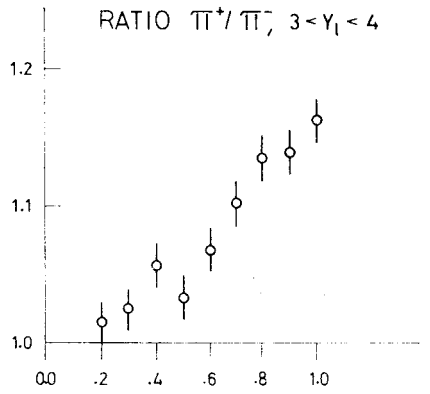

Fig. 17. The ratio of the production cross-section for π^+ to that of π^- in proton-proton collisions for $3<y_1(=y_{max}-y)<4$ as function of the transverse momentum, p_T. The centre-of-mass energies are 30.6 and 52.8 GeV. The data are from the BS-group, Ref. [26]

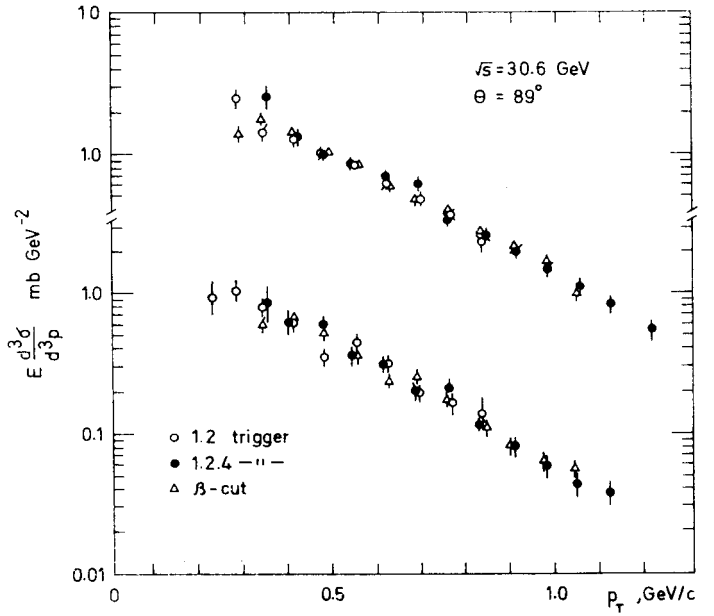

Fig. 18. The invariant cross-section for production of protons and antiprotons in proton-proton collisions of centre-of-mass energy 30.6 GeV as function of the transverse momentum p_T. Production angle $\Theta = 89°$. The three signs for the data represents different trigger-modes. The data are from the BS-group, Ref. [27]

(*v*) The cross-sections for kaons have been measured over a more limited range in p_T ($0.2 < p_T < 0.5$ GeV/*c*) and with less accuracy. Within the accuracy of the data they are consistent with a flat plateau as a function of y_1 for values of $y_1 > 3.4$ ($y_{1\,max} = 4.0$). They are also consistent with a rise similar to that of the pions.

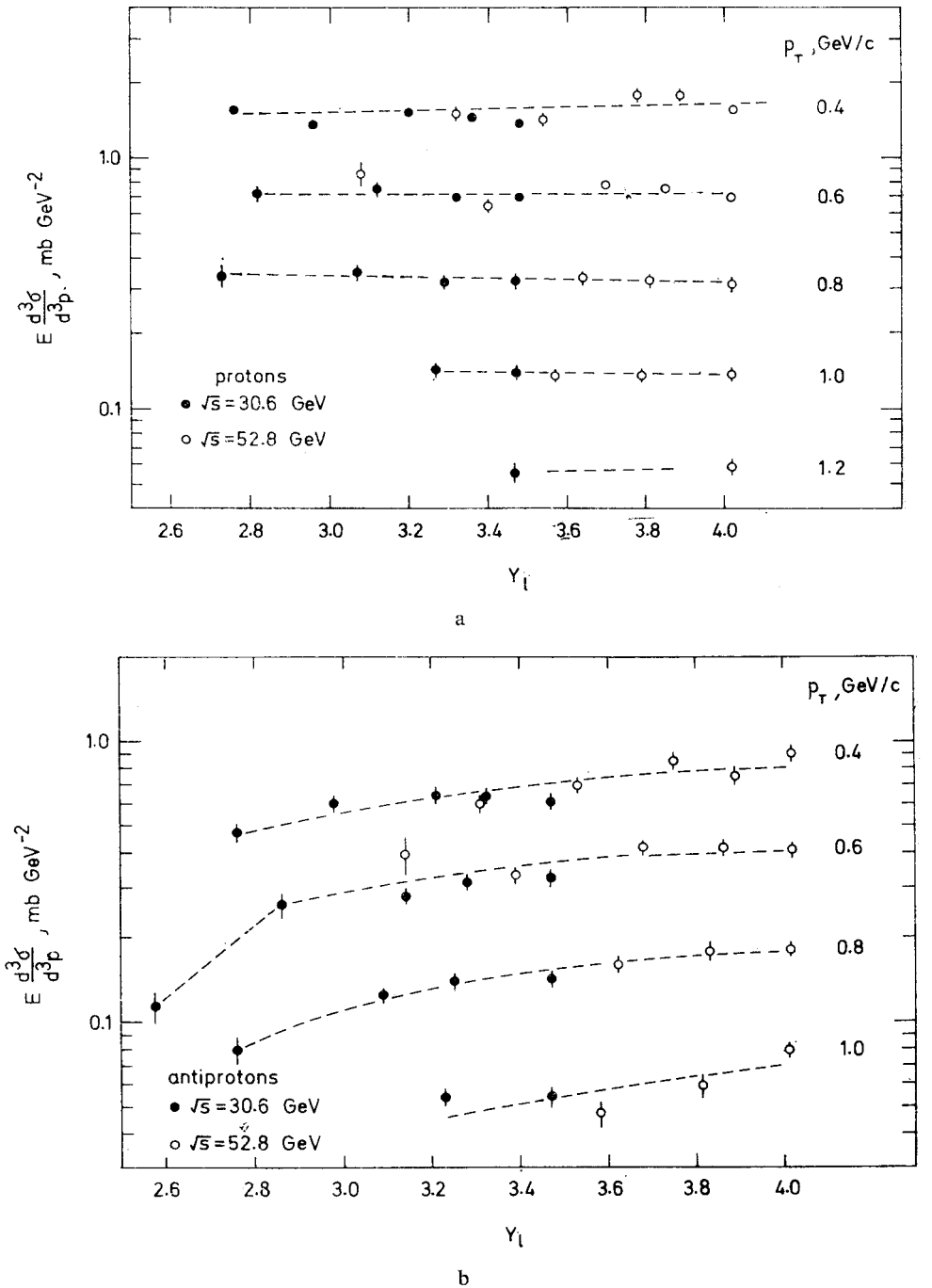

Fig. 19. The invariant cross-section for production of $p^{\pm}$ in proton-proton collisions of centre-of-mass energies 30.6 and 52.8 GeV as function of $y_1 = y_{max} - y$ for transverse momenta p_T = 0.4, 0.6, 0.8, 1.0 and 1.2 GeV/c. The data are from the BS-group, Ref. [27]

TABLE III

Parameters for the fits of the invariant cross-sections for $\pi^{\pm}$ to the forms $F = Ae^{-Bp_T}$ (Linear) and $F = Ae^{Bp_T+Cp_T^2}$ (Quadratic)

Particle	s, GeV	Θ_I	Range in p_T, GeV/c	Linear fit			Quadratic fit			
				A	B (GeV/c)$^{-1}$	$p(\chi^2)$	A	B (GeV/c)$^{-1}$	C (GeV/c)$^{-2}$	$p(\chi^2)$
π^+	30.6	89	0.13–1.05	149±3	6.04±.05	0.000	187±7	7.1±.1	1.0±.1	0.10
		75	0.13–1.00	154±4	6.05±.05	0.001	184±7	7.1±.2	1.0±.2	0.45
		62.5	0.12–0.95	150±5	6.13±.06	0.01	190±10	7.2±.2	1.0±.2	0.28
		45	0.11–0.75	145±5	6.30±.09	0.09	143±12	6.2±.4	−0.1±.5	0.08
		36	0.11–0.60	136±5	6.45±.10	0.65	150±2	7.1±1	1.0±.1	0.69
π^-	30.6	89	0.13–1.05	157±4	6.25±.05	0.000	203±9	7.5±.2	1.2±.2	0.40
		75	0.13–1.00	154±4	6.34±.05	0.03	178±10	7.0±.2	0.6±.2	0.14
		62.5	0.12–0.95	133±4	6.02±.06	0.000	174±12	7.3±.3	1.2±.3	0.01
		45	0.11–0.75	127±5	6.10±0.8	0.60	128±10	6.2±.4	0.1±.5	0.60
		36	0.11–0.60	146±5	6.9±.1	0.78	148±11	7.0±.5	0.1±.7	0.75
π^+	52.8	89	0.13–1.05	163±4	6.08±.05	0.000	212±9	7.3±.2	1.3±.2	0.30
		75	0.13–1.00	170±4	6.26±.05	0.000	207±10	7.3±.2	1.0±.2	0.01
		62.5	0.12–0.95	156±4	6.13±0.6	0.000	210±10	7.6±.2	1.6±.2	0.74
		45	0.11–0.75	144±5	6.16±.09	0.22	166±11	7.1±.4	1.2±.6	0.50
		36	0.11–0.60	139±9	6.04±.18	0.62	197±20	8.1±.6	2.7±.8	0.79
π^-	52.8	89	0.13–1.05	160±4	6.16±.05	0.007	197±8	7.2±.2	1.0±.2	0.75
		75	0.13–1.00	160±4	6.22±.05	0.006	182±8	6.9±.2	0.7±.2	0.06
		62.5	0.12–0.95	161±4	6.23±.05	0.15	186±8	7.0±.2	0.8±.2	0.61
		45	0.11–0.75	150±5	6.39±.09	0.82	152±10	6.4±.4	0.1±.5	0.82
		36	0.11–0.60	177±12	6.9±.2	0.98	169±33	7.5±.9	0.8±1.2	0.98

(*vi*) Within errors the ratio between the cross-sections for K^+ and K^- is 1.27 ± 0.3 for $0.2 < p_T < 0.5$ GeV/c.

(*vii*) The p_T spectra for protons and in particular for antiprotons tend to flatten off toward small p_T, in contrast to the pion spectra which rise essentially exponentially even for small values of p_T. This is shown most clearly by a fit of the data to $F = \exp(-Bp_T+Cp_T^2)$ where C becomes negative with a magnitude of the order of 0.5 (GeV/c)$^{-2}$ for protons and of the order of 2–3 (GeV/c)$^{-2}$ for antiprotons. The group does not rule out an unknown error in the background subtraction for protons which would mostly affect the data for low p_T and thus would give a wrong p_T dependence in this region. Uncertainties here should not exceed an additional 10%. The background is in general largest for the small angles. Fig. 18 shows a set of data for $\sqrt{s} = 30.6$ GeV and $\Theta_I = 89°$.

(*viii*) Fig. 19 shows the y-dependence of F for protons (a) and antiprotons (b) for several values of p_T for $\sqrt{s} = 30.6$ and 52.8 GeV. It is seen that the proton cross-sections are consistent with having reached a plateau. The antiproton data on the other hand are

still increasing with y and with some goodwill one may see that the slope of F in the neighbourhood of y_{max} for each energy (3.48 and 4.03 for $\sqrt{s} = 30.6$ and 52.8 GeV respectively) tends to zero.

Tables of the data will be found in Refs [25–27].

To summarize some of the findings for the inclusive production of $\pi^{\pm}$, $K^{\pm}$ and $p^{\pm}$ I include Figures 20 and 21.

Fig. 20 shows a collection of data from the CHLM, BCC, BS and SS groups for $p_T = 0.4$ GeV/c, from many ISR energies, and from the experiment of Mück *et al.* for

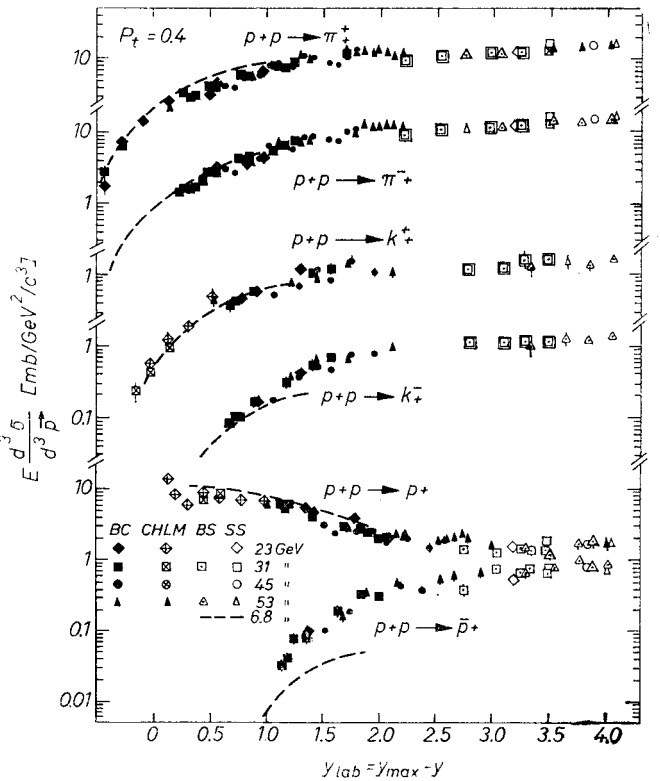

Fig. 20. The invariant cross-section for production of π^+, K^+ and $p^{\pm}$ in proton-proton collisions of centre-of-mass energies as indicated in the figure, as function of $y_1 = y_{max} - y$. A compilation of data from the BC, BS, CHLM and SS-groups. The dashed lines indicate the data of Mück *et al.*, Ref. [28]

$\sqrt{s} = 6.8$ GeV. The figure in itself summarizes the scaling behaviour for all the six particle types discussed. I shall only point out the structure in the pion data around $y_1 = 1.5-2.5$. It is not clear whether the data from the BCC group and the BS group here show a structure or only the uncertainty in the absolute accuracy of the data.

Fig. 21 shows what the scaling features look like for π^+ for $p_T = 0.8$ GeV, but now plotted as a function of x, summarizing some of the data from the BCC, BM [31], BS and the CHLM groups together with data from Allaby *et al.* [21].

Production of particles with large transverse momentum

Recent results on production of charged particles and/or π^0 at the ISR come from the CCR [32], BS [33, 34] and the SS [35] groups. The CCR-data on π^0 production at $\Theta = 90°$ with $p_T \lesssim 8$ GeV/c are still preliminary and essentially those published last fall at the Batavia conference. The data from the BS group are partly on cross-sections for total positive and total negative particles at $\Theta = 89°$ and 59.4°, up to $p_T \sim 5$ GeV/c [33], partly on particle ratios at $\Theta = 89°$ for $1.4 < p_T < 3.5$ GeV/c. The SS-data are taken

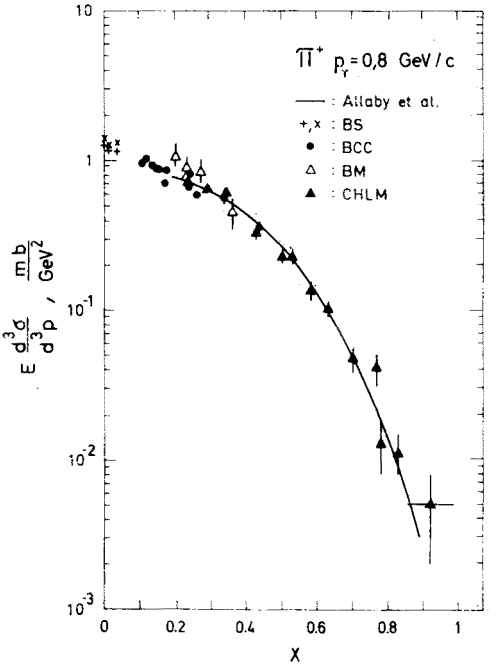

Fig. 21. The invariant cross-section for production of π^+ of transverse momentum $p_T = 0.8$ GeV/c in proton-proton collisions of varying (ISR-) centre-of-mass energies as function of $x = 2p_L/\sqrt{s}$. The line represents the data of Allaby *et al.*, Ref. [21]. The data points are from the BCC, BM, BS and CHLM groups

at $\Theta = 90°$ and cover cross-sections for all positive or all negative particles up to $p_T = 3$ GeV/c for all the four ISR energies, some data on π^0 production up to $p_T = 2.5$ GeV/c and separated π^+ and π^- cross-sections for $\sqrt{s} = 44.7$ and 52.8 GeV in the interval $3 \lesssim p_T \lesssim 5$ GeV/c.

The, by now, well known feature of these data is that the invariant cross-section, as function of p_T, does not continue its exponential fall-off with p_T, but flattens off such that a linear exponential fit to the pion cross-sections for $3.5 < p_T < 5.0$ GeV/c gives $B \sim 2.4$ (GeV/c)$^{-1}$, to be compared to $B \sim 6.0$ (GeV/c)$^{-1}$ for $p_T < 1.0$ GeV/c [35].

If one tries to get more detailed information out of these data-sets one discovers

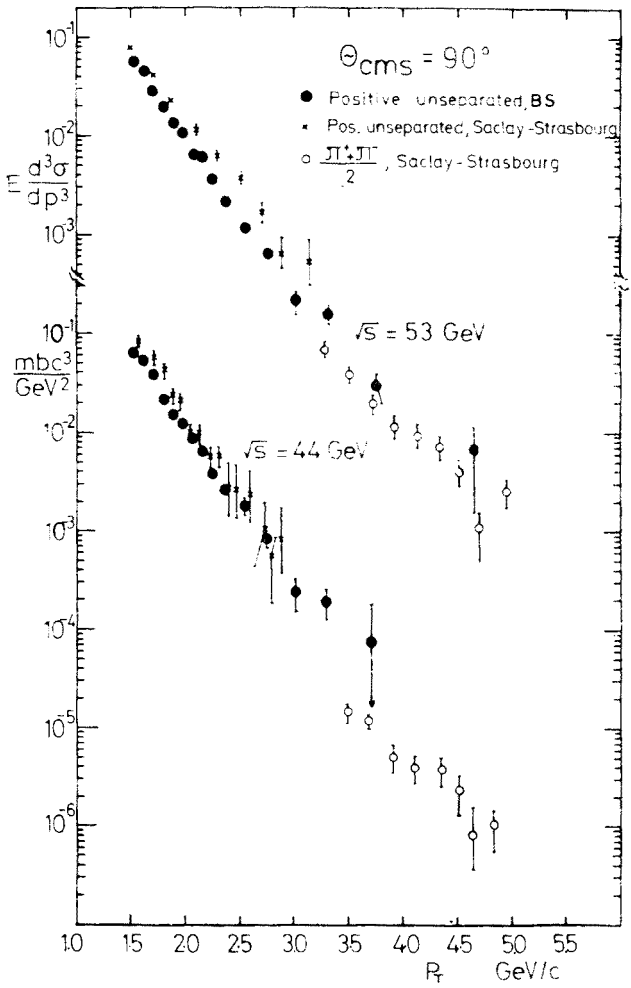

Fig. 22. The invariant cross-section for production of charged particles at 90° in proton-proton collisions of centre-of-mass energies 44.7 and 52.8 GeV as function of transverse momentum, p_T. Data on positive unseparated particles is by the BS and the SS-groups and data on the added cross-section for positive and negative pions from the SS-group. See Ref. [33] and [25]

some inconsistencies, and it may be advisable therefore to wait for more accurate data for separated charged particles which are being recorded at present.

I shall still comment on some points:

(*i*) A strong energy dependence has been found by the SS-group, (*e.g.* for $p_T = 2.5$ GeV/c an increase by about 70% from $\sqrt{s} = 44.7$ to 52.8 GeV) but the BS group finds essentially no such energy dependence ($\lesssim 20\%$ in the same case). See Fig. 22.

(*ii*) For $2.0 < p_T < 3.0$ GeV/c the SS group reports a cross-section for all positive particles about four times that for π^0, but the π^0 cross-section reported by the CCR group

TABLE IV

Particle ratios at $\Theta = 90°$

Ratio	30.6 GeV		44.7 GeV	
	$p_T = 1.4-2.0$ GeV/c	2.0–3.5	1.4–2.0	2.0–3.5
π^+/all	0.34 ± 0.02	0.31 ± 0.04	0.33 ± 0.02	0.30 ± 0.04
π^-/all	0.29 ± 0.02	0.25 ± 0.03	0.32 ± 0.02	0.25 ± 0.03
K^+/all	0.26 ± 0.02	0.14 ± 0.02	0.22 ± 0.02	0.16 ± 0.03
p/all		0.16 ± 0.03		0.12 ± 0.02
K^-/all	0.11 ± 0.01	0.10 ± 0.02	0.13 ± 0.01	0.11 ± 0.02
$\bar{}$/all		0.05 ± 0.02		0.07 ± 0.02
π^-/π^+	0.87 ± 0.06	0.79 ± 0.09	0.99 ± 0.08	0.84 ± 0.10
$(K^+ + p)/\pi^+$	0.78 ± 0.06	0.94 ± 0.10	0.66 ± 0.06	0.91 ± 0.10
$(K^- + \bar{p})/\pi^-$	0.38 ± 0.04	0.59 ± 0.09	0.41 ± 0.04	0.70 ± 0.10
all$^+$/all$^-$	1.48 ± 0.10	1.53 ± 0.15	1.19 ± 0.08	1.33 ± 0.13

in the interval $2.5 < p_T < 3.5$ GeV/c for $\sqrt{s} = 52.8$ GeV is higher than one half the cross-section for all charged particles as measured by the BS group (see Fig. 23) or about equal to the π^+ or π^- cross-section measured by the SS group.

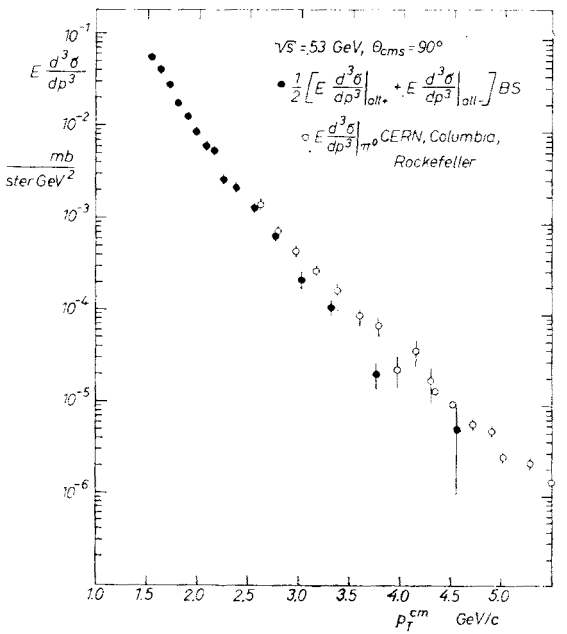

Fig. 23. The invariant cross-section for production of charged particles and π^0 at 90° in proton-proton collisions of centre-of-mass energies 52.8 GeV as function of the transverse momentum, p_T. Data on π^0 are from the CCR-group, Ref. [32], those on charged particles from the BS-group, Ref. [33]

(*iii*) Table IV shows the particle composition for two intervals of p_T for $\sqrt{s} = 30.6$ and 44.7 GeV. There is relatively little energy dependence, but the ratio of positive to negative particles decreases, as would be expected from the increase in particle multiplicity.

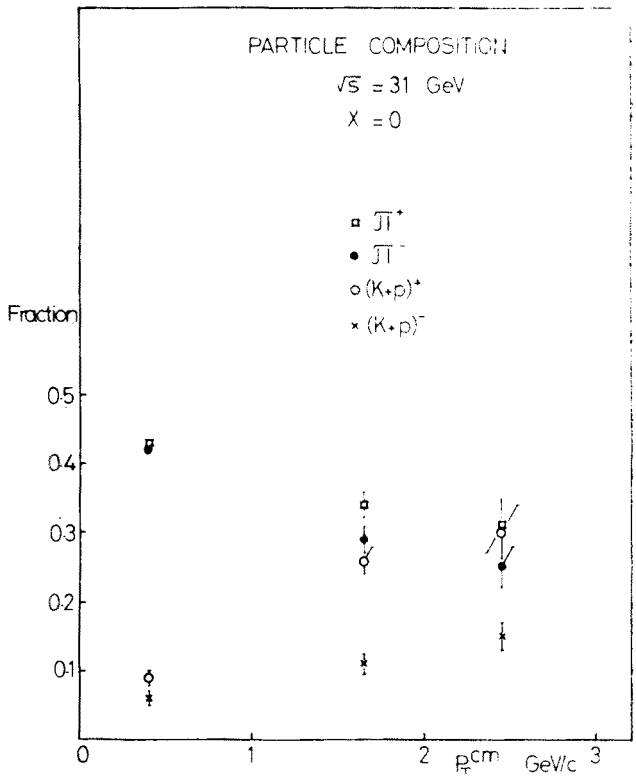

Fig. 24. The fraction of π^+, π^-, $(K+p)^+$ and $(K+p)^-$ in the total of charged particles produced at 90° in proton-proton collisions of centre-of-mass energy 31 GeV as function of the transverse momentum, p_T. The data are from the BS group, Ref. [34]

The contents of heavier particles increases with increasing transverse momentum (see Fig. 24), showing that also for the larger p_T values the invariant cross-section for the heavier particles has a slower decrease with p_T than for the light particles.

Search for heavy or unknown particles

It is rather easy to report on the search for quarks and magnetic monopoles. No real candidate has bee seen. As far as quarks are concerned, the BS group [36] reports this negative result in the form of upper limits as shown in Fig. 25. Out of $7 \cdot 10^7$ charged particles going through the BS spectrometer, which had been tuned to record only slow particles $0.2 < \beta < 0.65$ and with $p > 0.9$ GeV/c, no quarks of charge $\frac{2}{3}e$ was seen. As far as I can understand the theoreticians today are happy as long as we don't find the quarks. The negative result must therefore be said to be positive.

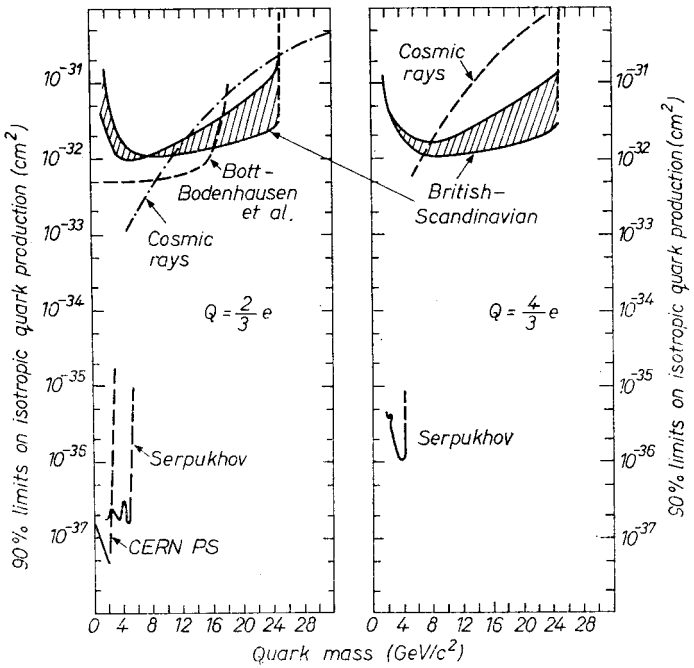

Fig. 25. Limits at 90% confidence level for production of quarks of charge $\frac{2}{3}e$ and $\frac{4}{3}e$ at $\Theta = 59°$ in proton-proton collisions of centre-of-mass energy 52.8 GeV. The limits are computed assuming an isotropic distribution of quarks in the cm-system. The data are from the BS-group, Ref. [36], where also references to data included for comparison are given

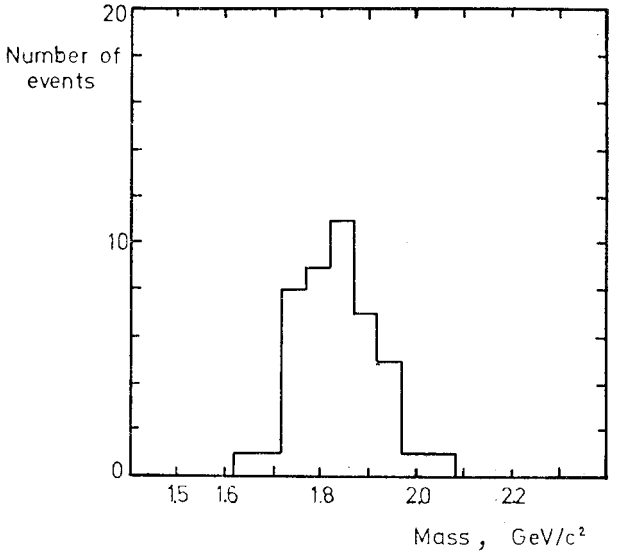

Fig. 26. Number of antideuterons observed in proton-proton collisions of centre-of-mass energy 52.8 GeV as function of the measured particle mass. Data from the BS-group, Refs [25] and [36]

A byproduct of the quark-search was the recording of deuterons and antideuterons. Deuterons are also knocked out of the vacuum-chamber walls producing a difficult background-subtraction problem. Antideuterons however, are not produced in beam-wall collisions and the resulting particles stand out clearly, both in their mass-value 1.88 GeV/c^2 (see Fig. 26) and in their origin from the diamond.

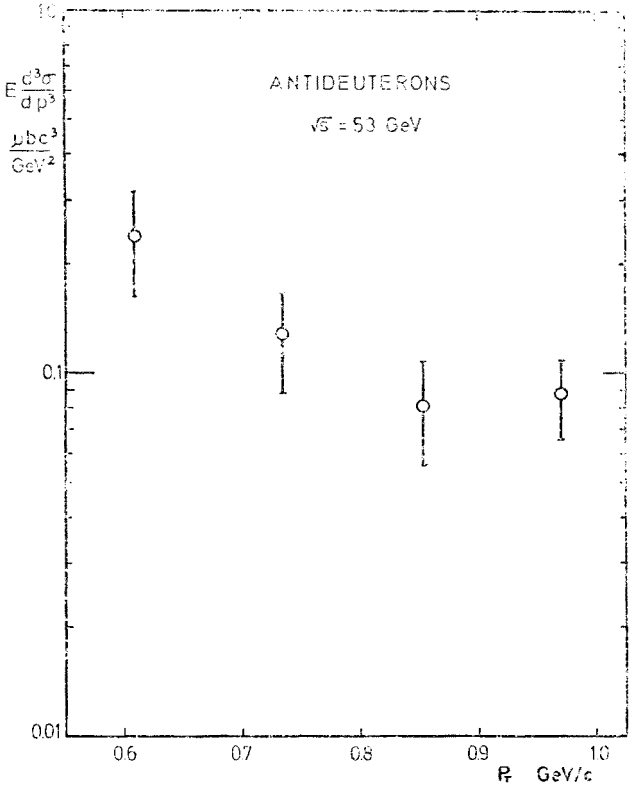

Fig. 27

A p_T spectrum for the d-production cross-section, recorded for $\sqrt{s} = 52.8$ GeV and $\Theta = 59°$, is shown in Fig. 27. Note that the scale is in μb/GeV^2.

It may be even more interesting to plot these data as function of $\sqrt{p_T^2+m^2}$, and compare with the invariant cross-section for producing other particles. This is done in Fig. 28, all data taken for $\sqrt{s} = 52.8$ GeV and $\Theta = 59°$. This parametrization does not help much in bringing a system into the production cross-sections, except maybe the fact that antideuterons and antiprotons in these intervals have cross-sections consistent with the same exponential $\sqrt{p_T^2+m^2}$ dependence, namely

$$F \sim 400\, e^{-8.3\sqrt{p_T+m^2}} \quad \text{(coarse hand-fit)}.$$

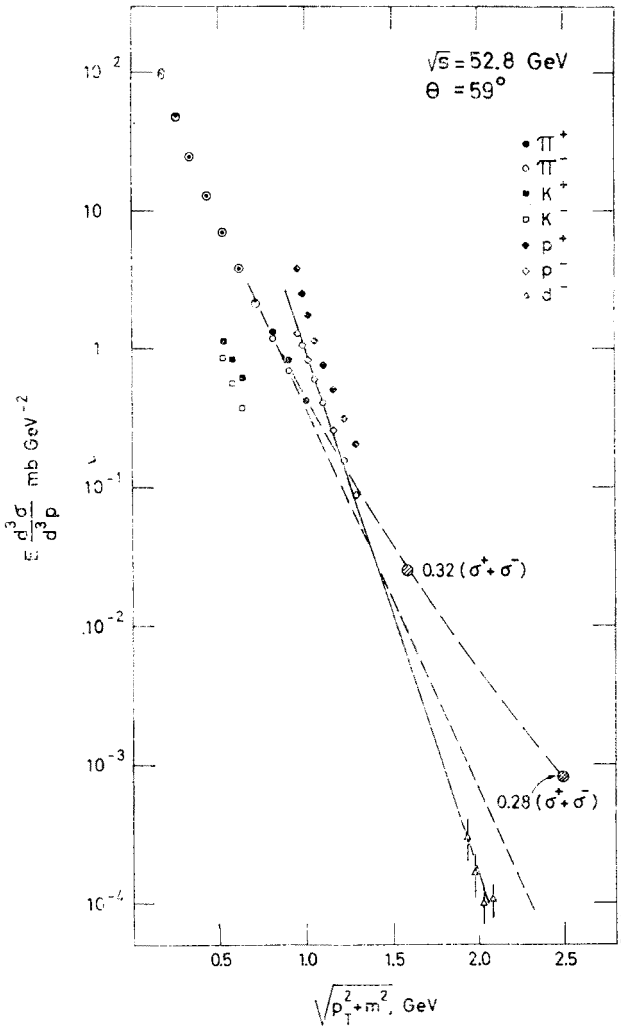

Fig. 28. The invariant cross-section for production of $\pi^{\pm}$, $K^{\pm}$, $p^{\pm}$ and d^- at $\Theta = 59°$ in proton-proton collisions of centre-of-mass energy 52.8 GeV as function of $\sqrt{p_T^2+m^2}$. The dashed curve connects the pion points of low p_T with two pion points estimated as 0.32 and 0.28 times the cross-sections for production of charged particles at $p_T = 1.6$ and 2.5 GeV/c respectively. The data are from the BS-group

In 1969 it was reported [37, 38] that d^- production in proton-aluminium collisions at incident proton momenta of 70 and 52 GeV occured with a rate about 10^{-5} times that of p^- for forward angles. They found the ratio $R(d^-)/R^2(p^-)$ to be approximately constant, varying between $2 \cdot 10^{-3}$ and $6 \cdot 10^{-3}$. R is here the rate compared to π^- production under the same conditions. In the present case, with $p_l = 1480$ GeV/c, in proton-proton collisions producing d^- at $\Theta = 59°$ the ratio is almost the same, about $5 \cdot 10^{-3}$. This shows an interesting consistency between the probability of producing antinucleons and antinuclei.

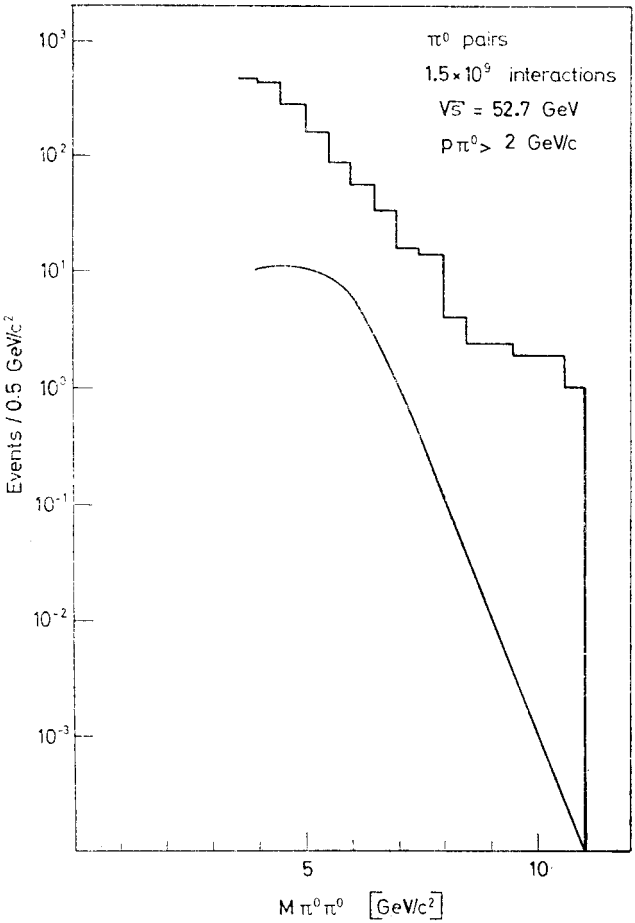

Fig. 29. π^0 pair events from proton-proton collisions of centre-of-mass energy 52.8 GeV as function of the $\pi^0\pi^0$ mass. The π^0's have both a momentum greater than 2 GeV/c and go into the angular range $60° < \Theta < 120°$ in opposite hemispheres. The data are from the CCR group, Ref. [32]

Correlations

Measurements of correlations between particles produced at the ISR have only barely started. Some of the results [39] have been discussed in another session at this school and I shall only comment on the experiments of the CCR [32] group and the CHLM group [40].

The CCR group has studied the $\pi^0\pi^0$-correlations when both particles have $p_T > 2\,\mathrm{GeV}/c$ and are emitted around $\Theta = 90°$, but into opposite detectors. This means that the angle between the particles is $60° \lesssim \Theta \lesssim 120°$. Fig. 29 shows the mass distributions of the $\pi^0\pi^0$ systems, compared with a distribution computed under the assumptions that the probability of observing a π^0 in one detector is independent of the observation of a π^0 in the other detetcor, and that each π^0 has a momentum distribution given by the experimental in-

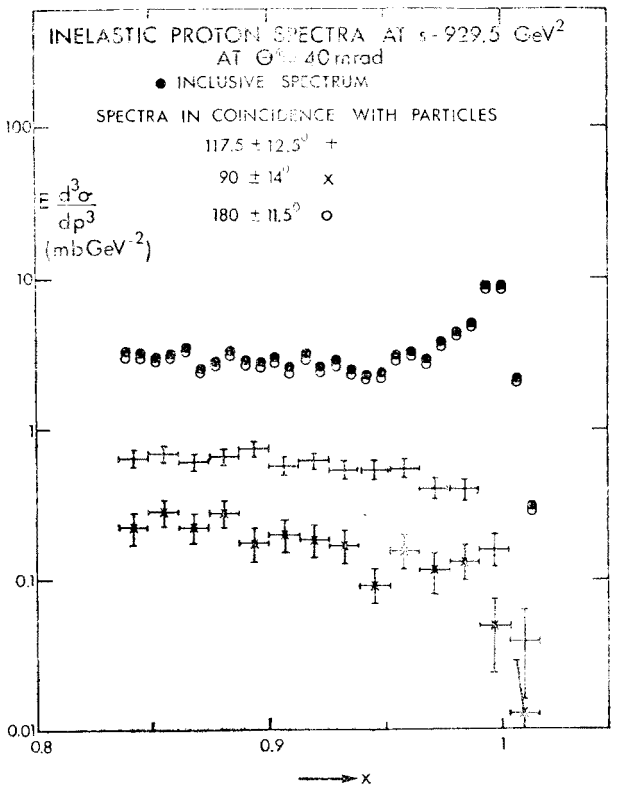

Fig. 30. The invariant cross-section for inelastic protons at $\Theta = 40$ mrad from proton-proton collisions of centre-of-mass energy 306 GeV as function of $x = 2p_L/\sqrt{s}$ (solid circles). Open circles represent protons in coincidence with other charged particles within a cone of halfangle about 11.°5 around the opposite direction to the inelastic proton momentum. Single crosses and double crosses refer to protons in coincidence with particles at 117,°5 and 90° respectively with respect to the direction of the incident beam 1 particle (see Fig. 11). The data are from the CHLM group, Ref. [40]

clusive π^0 distributions measured by the same group. Momentum conservation has not been included in the calculations, and it is therefore not clear whether the rather large correlation between the π^0's come from such kinematical effects or from other effects.

By modifying their experimental setup for measuring single particle inclusive production in the small angle region the CHLM group has studied correlations in inelastic events with $x \sim 1$ [20, 40]. The modified setup is shown in Fig. 11. Three counter telescopes are added to the spectrometer:

1. A telescope below the diamond, subtending the angular interval $76° < \Theta < 104°$.
2. A telescope in the horizontal plane, $15° < \Theta < 130°$.
3. A telescope around beam 2, covering most of the angular range up to $\Theta = 200$ mrad.

The results are shown in Fig. 30 and clearly demonstrate that with almost all inelastic protons with $x > 0.85$ there is at least one accompanying charged particle within a cone with half-angle 200 mrad around beam 2. It is also clear that a great fraction of these

events include particles emitted at large angles, with a minimum around 90°. The fraction of inelastic events with particles emitted into the telescopes is essentially constant for $0.85 < x < 0.96$. As x increases beyond this value the percentage of additional forward particles stays constant, but for the larger angles the percentage quickly drops toward 0.

This picture looks reasonable: An isobar or a light cluster of particles come out of the "contact" with the other proton, and when the proton has given away only very little energy, the other proton has been very little excited and its "decay" products must follow within a relatively narrow cone.

As was pointed out to me during the lecture, it may be more surprising that even for x-values as high as 0.98 a large fraction of the events include particles going into the central region. The ratio of the invariant cross-section for inclusive proton production at $x \sim 0.98$ to the cross-section for producing such a proton and a charged particle at large angles is about 0.02 for telescope 1 ($\Theta \sim 90^0$) and about 0.12 for telescope 2 ($\Theta \sim 117^0$, 5).

The group finds that for protons with $x > 0.99$, $\langle n_{ch} \rangle = 2.8 \pm 0.5$ and for protons with $0.72 < x < 0.84$, $\langle n_{ch} \rangle = 6.7 \pm 1.5$.

The above examples on particle correlations are rather simple. In the future we will look forward to more and more data on correlations in high energy collisions, both measured at the ISR anp at NAL. These data will be complicated to analyse, and I think it will be extremely important to keep a close contact between experimentalists and theoreticians in these studies. The Cracow Summer School is one place through which such contacts will continually be made, but one will need more. One will need theoreticians working with the experimentalists during the entire experiments.

In conclusion I should like to express my thanks to Professor A. Białas and the organizing committee for inviting me to this school and for their most warmhearted hospitality during this time.

REFERENCES

[1] K. Johnsen, *Nuclear Instrum. Methods*, **108**, 205 (1973).
[2] P. J. Carlsen, O. Leistam, University of Stockholm *report* USIP-71-11.
[3] E. Fermi, *Progr. Theor. Phys.*, **5**, 570 (1950).
[4] R. Hagedorn, J. Ranft, *Nuclear Phys.*, **B48**, 157 (1972) *etc.*
[5] L. D. Landau, *Izv. Akad. Nauk SSSR*, **17**, 51 (1953), English translation in Collected Papers of L. D. Landau, ed. D. TerHaar, Gordon and Breach, New York 1965, p. 569.
[6] P. Carruthers, Minh Duong-van, Cornell University *report* CLNS-212.
[7] D. Amati, S. Fubini, A. Stanghellini, *Nuovo Cimento*, **26**, 896 (1962).
[8] R. P. Feynman, *Phys. Rev. Letters*, **23**, 1415 (1969).
[9] J. Benecke, T. T. Chou, C. N. Yang, E. Yen, *Phys. Rev.*, **188**, 2159 (1969).
[10] U. Amaldi, R. Biancastelli, C. Bosio, G. Matthiae, J. V. Allaby, W. Bartel, M.M. Block, G. Cocconi, A. N. Diddens, R. W. Dobinson, J. Litt, A. M. Wetherell, *Phys. Letters*, **43B**, 231 (1973); U. Amaldi, R. Biancastelli, C. Bosio, G. Matthiae, J. V. Allaby, W. Bartel, G. Cocconi, A. N. Diddens, R. W. Dobinson, A. M. Wertherell, *Phys. Letters*, **44B**, 112 (1973).
[11] S. R. Amendolia, G. Bellettini, P. L. Braccini, C. Bradaschia, R. Castaldi, V. Cavasinni, C. Cerri, T. Del Prete, L. Foa, P. Giromini, P. Laurelli, A. Menzione, L. Ristori, G. Sanguinetti, M. Valdata, G. Finocchiaro, P. Grannis, D. Green, R. Mustard, R. Thun, *Phys. Letters*, **44B**, 119 (1973) and paper submitted to *Nuovo Cimento*.

[12] M. Holder, E. Rademacher, A. Staude, G. Barbiellini, P. Darriulat, M. Hansroul, S. Orito, P. Palazzi, A. Santroni, P. Strolin, K. Tittel, J. Pilcher, C. Rubbia, G. De Zorzi, M. Macri, G. Sette, C. Grosso-Pilcher, A. Fainberg, G. Maderni, *Phys. Letters*, **35B**, 361 (1971).

[13] M. Froissart, *Phys. Rev.*, **123**, 1053 (1961).

[14] M. Holder *et al.*, (see Ref. [12]), *Phys. Letters*, **35B**, 355 (1971); **35B**, 361 (1971); **36B**, 400 (1971); G. Barbiellini, M. Bozzo, P. Darriulat, G. Diambrini Palazzi, G. De Zorzi, A. Fainberg, M. I. Ferrero, M. Holder, A. McFarland, G. Maderni, S. Orito, J. Pilcher, C. Rubbia, A. Santroni, G. Sette, A. Staude, P. Strolin, K. Tittel, *Phys. Letters*, **39B**, 663 (1972).

[15] U. Amaldi, R. Biancastelli, C. Bosio, G. Matthiae, J. V. Allaby, W. Bartel, G. Cocconi, A. N. Diddens, R. W. Dobinson, V. Elings, J. Litt, L. S. Rochester, A. M. Wetherell, *Phys. Letters*, **36B**, 504 (1971) and submitted to *Phys. Letters*.

[16] G. Bellettini, P. L. Braccini, C. Bradaschia, R. Castaldi, T. Del Prete, L. Foa, P. Giromini, P. Laurelli, A. Menzione, M. Valdata, G. Finocchiaro, P. Grannis, D. Green, R. Mustard, R. Thun, submitted to *Phys. Letters*.

[17] J. Babecki, Z. Chyliński, Z. Czachowska, O. Czyżewski, B. Furmańska, J. Gierula, R. Holyński, A. Jurak, K. Karnicka, S. Krzywdziński, G. Nowak, W. Wolter, A. Gurtu, A. J. Herz, *Phys. Letters*, **40B**, 507 (1972).

[18] M. G. Albrow, A. Bagchus, D. P. Barber, A. Bogaerts, B. Bosnjakovic, J. R. Brooks, A. B. Clegg, F. C. Erné, C. N. P. Gee, D. H. Locke, F. K. Loebinger, P. G. Murphy, A. Rudge, J. C. Sens, F. Van der Veen, submitted to *Nuclear Phys.*

[19] M. G. Albrow, D. P. Barber, A. Bogaerts, B. Bosnjakovic, J. R. Brooks, A. B. Clegg, F. C. Erné, C. N. P. Gee, A. D. Kanaris, A. Lacourt, D. H. Locke, F. K. Loebinger, P. G. Murphy, A. Rudge, J. C. Sens, K. Terwilliger, F. Van der Veen, *Phys. Letters*, **42B**, 279 (1972).

[20] M. G. Albrow *et al.* (see Ref. [18]), *Nuclear Phys.*, **B54**, 6 (1973).

[21] J. V. Allaby, A. N. Diddens, R. W. Dobinson, A. Klovning, J. Litt, L. S. Rochester, K. Schlüpmann, A. M. Wetherell, U. Amaldi, R. Biancastelli, C. Bosio, G. Matthiae, *Contribution to the 4th International Conference on High Energy Collisions*, Oxford 1972.

[22] M. G. Albrow, D. P. Barber, A. Bogaerts, B. Bosnjakovic, J. R. Brooks, A. B. Clegg, F. C. Erné, C. N. P. Gee, A. D. Kanaris, D. H. Locke, F. K. Loebinger, P. G. Murphy, A. Rudge, J. C. Sens, K. Terwilliger, F. van der Veen, *Nuclear Phys.*, **B51**, 388 (1973).

[23] M. Antinucci, A. Bertin, P. Capiluppi, G. Giacomelli, A. M. Rossi, G. Vinnini, A. Bussiere, presented at the *Int. Conf. on New Results from Exp. on High-Energy Particle Collisions*, Nashville 1973.

[24] G. Giacomelli, private communication.

[25] B. Alper, H. Bøggild, P. Booth, F. Bulos, L. J. Carroll, G. Von Dardel, G. Damgaard, B. Duff, J. N. Jackson, G. Jarlskog, L. Jønsson, A. Klovning, L. Leistam, E. Lillethun, G. Lynch, M. Prentice, D. Quarrie, J. M. Weiss, presented by G. Jarlskog at the *Int. Conf. on New Results from Exp. on High-Energy Collisions*, Nashville 1973.

[26] B. Alper *et al.* (see Ref. [25]), *Large Angle Inclusive Production of Charged Pions at the CERN ISR with Transverse Momenta Less Than 1.0 GeV/c*, to be published.

[27] B. Alper *et al.* (see Ref. [25]), *Inclusive Production of Protons, Antiprotons and Kaons and Particle Composition at Small x at the CERN ISR*, to be published.

[28] H. J. Mück, M. Schatter, F. Selonke, W. Wessels, V. Blobel, A. Brandt, G. Drews, H. Fesefeldt, B. Hellwig, D. Mönkenmeyer, P. Söding, G. W. Brandenburg, H. Franz, P. Freund, D. Luers, W. Richter, W. Schrankel, *Phys. Letters*, **39B**, 303 (1972).

[29] T. Ferbel, *Phys. Rev. Letters*, **29**, 448 (1972).

[30] M. Banner, J. L. Hamel, J. P. Pansart, A. V. Stirling, J. Teiger, H. Zaccone, J. Zsembery, G. Bassompierre, M. Croissiaux, J. Gresser, R. Morand, M. Riedinger, M. Schneegans, *Phys. Letters*, **41B**, 547 (1972).

[31] L. G. Ratner, R. J. Ellis, G. Vannini, B. A. Babcock, A. D. Krisch, J. B. Roberts, *Phys. Rev. Letters*, **27**, 68 (1971).

[32] F. W. Büsser, L. Camilleri, L. DiLella, G. Gladding, A. Placci, B. G. Pope, A. M. Smith, J. K. Yoh, E. Zavattini, B. J. Blumenfeld, L. M. Lederman, R. L. Cool, L. Litt, S. L. Segler, presented at the *Int. Conf. on New Results from Exp. on High-Energy Particle Collisions*, Nashville 1973.

[33] B. Alper, H. Bøggild, G. Jarlskog, G. Lynch, J. M. Weiss, P. Booth, L. J. Carroll, J. N. Jackson, M. Prentice, G. von Dardel, L. Jønsson, G. Damgaard, K. H. Hansen, E. Lohse, F. Bulos, L. Leistam, A. Klovning, E. Lillethun, B. Duff, F. Heymann, D. Quarrie, *Phys. Letters*, **44B**, 521 (1973).

[34] B. Alper, H. Bøggild, G. Jarlskog, J. M. Weiss, P. Booth, L. J. Carroll, J. N. Jackson, M. Prentice, G. von Dardel, G. Damgaard, F. Bulos, W. Lee, G. Manning, P. Sharp, L. Leistam, A. Klovning, E. Lillethun, B. Duff, K. Potter, D. Quarrie, S. Sharrock, *Phys. Letters*, **44B**, 527 (1973).

[35] M. Banner, J. L. Hamel, J. P. Pansart, A. V. Stirling, J. Teiger, H. Zaccone, J. Zsembery, G. Bassompierre, M. Croissiaux, J. Gresser, R. Morand, M. Riedinger, M. A. Schneegans, *Phys. Letters*, **44B**, 537 (1973).

[36] B. Alper, H. Bøggild, P. Booth, F. Bulos, L. J. Carroll, G. von Dardel, G. Damgaard, B. Duff, F. Heymann, J. N. Jackson, G. Jarlskog, L. Jønsson, A. Klovning, L. Leistam, E. Lillethun, G. Lynch, G. Manning, M. Prentice, D. Quarrie, J. M. Weiss, to be published.

[37] E. Lillethun, *Proceedings of the Lund Int. Conf. on Elementary Particles*, 1969, p. 167.

[38] F. Binon, P. Duteil, V. A. Kachanov, V. P. Khromov, V. M. Kutyin, V. G. Lapshin, J. P. Peigneux, Yu. D. Prokoshkin, E. A. Razuvaev, V. I. Rykalin, R. S. Shuvalov, V. I. Solianik, M. Spighel, J. P. Stroot, N. K. Vishnevsky, *Phys. Letters*, **30B**, 510 (1969).

[39] H. Dibon, G. Flügge, Ch. Gottfried, B. M. K. Nefkens, G. Neuhofer, F. Niebergall, M. Regler, W. Schmidt-Parzefall, K. R. Schubert, P. E. Schumacher, K. Winter, submitted to *Phys. Letters*.

[40] M. G. Albrow, A. Bagchus, D. P. Barber, A. Bogaerts, B. Bosnjakovic, J. R. Brooks, A.B. Clegg, F. C. Erné, C. N. P. Gee, D. H. Locke, F. K. Loebinger, P. G. Murphy, A. Rudge, J. C. Sens, *Phys. Letters*, **44B**, 207 (1973).